

The crystal chemistry of the gedrite-group amphiboles. I. Crystal structure and site populations

M. SCHINDLER¹, E. SOKOLOVA¹, Y. ABDU¹, F. C. HAWTHORNE^{1,*}, B. W. EVANS² AND K. ISHIDA³

¹ Department of Geological Sciences, University of Manitoba, Winnipeg, Manitoba, Canada R3T 2N2

² Department of Earth and Space Sciences, University of Washington, Box 351310, Seattle, Washington 98195, USA

³ Department of Evolution of Earth Environments, Graduate School of Social and Cultural Studies, Kyushu University, 4-2-1 Ropponmatsu, Chu-ku, Fukuoka 810-8560, Japan

[Received 11 April 2008; Accepted 11 August 2008]

ABSTRACT

The crystal structures of twenty-five orthorhombic Fe-Mg-Mn amphiboles, $a = 18.525\text{--}18.620$, $b = 17.806\text{--}18.034$, $c = 5.264\text{--}5.303$ Å, $V = 1737.6\text{--}1776.7$, space group = $Pnma$, $Z = 4$, have been refined to R indices in the range 2.1–7.8% using 790–1804 unique observed reflections measured with Mo- $K\alpha$ X-radiation on a Bruker $P4$ automated four-circle diffractometer equipped with a 1K CCD detector. The quality of the refinements is strongly a function of the $^{[4]}Al$ content of the crystals because of unmixing in the central part of the series due to the presence of a low-temperature solvus. The amphibole crystals were analysed by electron microprobe subsequent to collection of the X-ray intensity data and span the anthophyllite–gedrite series from 0.17–1.82 $^{[4]}Al$ a.p.f.u. Mössbauer spectroscopy shows that the amphiboles of this series commonly contain small but significant amounts of Fe^{3+} . The amount of $^{[4]}Al$ is linearly related to the grand $\langle T-O \rangle$ distance by the equation $\langle T-O \rangle = 1.6214 + 0.171 \, ^{[4]}Al$, $R = 0.980$; the slope of this relation is not significantly different from that characteristic of a hard-sphere model. The $\langle T-O \rangle$ distances indicate the following site preference for $^{[4]}Al$: $T1B > T2B > T1A >> T2A$. The $\langle M2-O \rangle$ distances are compatible with all $^{[6]}Al$ and Fe^{3+} ordered at the $M2$ site. The grand $\langle M^{1,2,3}-O \rangle$ distance is related to the mean radius of the constituent cations, $\langle r^{M^{1,2,3}} \rangle$, by the equation $\langle \langle M^{1,2,3}-O \rangle \rangle = 1.4684 + 0.8553(7) \langle r^{M^{1,2,3}} \rangle$.

KEY WORDS: anthophyllite, gedrite, orthorhombic amphibole, crystal-structure refinement, electron-microprobe analysis, Mössbauer spectroscopy, site populations.

Introduction

THERE has been much less work done on the crystal chemistry of the orthorhombic amphiboles than on the monoclinic amphiboles. To some extent, this reflects the less frequent occurrence of the orthorhombic amphiboles. Furthermore, the common orthorhombic amphiboles show exsolution features that complicate crystallographic and spectroscopic work. Here, we try to remedy this situation through a systematic examination of the crystal chemistry of the $Pnma$ amphiboles of the

anthophyllite–gedrite series. A view of the $Pnma$ amphibole structure is shown in Fig. 1, and should be used in conjunction with the discussion throughout this paper.

Previous work

Crystal structure

The crystal structure of anthophyllite was solved by Warren and Modell (1930), who showed that the structure is based on amphibole double-chains with a staggered stacking of layers in the c direction such that the symmetry is orthorhombic (e.g. Ito and Morimoto, 1950), and that the structure contains essential (OH). Lindemann

* E-mail: frank_hawthorne@umanitoba.ca
DOI: 10.1180/minmag.2008.072.3.703

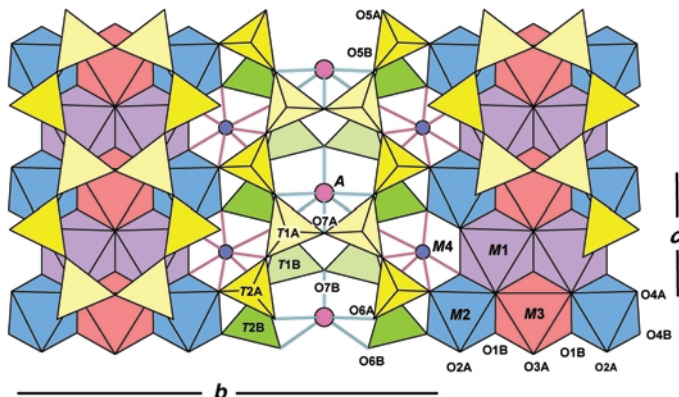


FIG. 1. The *Pnma* amphibole structure projected onto (100); polyhedra: *T*1*A*, pale yellow; *T*1*B*, bright yellow; *T*2*A*, pale green; *T*2*B*, bright green; *M*1, mauve; *M*2, blue; *M*3, rose; sites: *M*4, blue circle; *A*, pink.

(1964) reported a refinement of the structure of anthophyllite. Finger (1970) and Walitzki *et al.* (1989) also refined the structure of two anthophyllites and presented site populations. Papike and Ross (1970) refined the structures of two gedrites and assigned site populations to both the *M* and the *T* sites. Evans *et al.* (2001) refined the structure of ten unheated and heat-treated crystals of anthophyllite at a variety of temperatures and presented site populations.

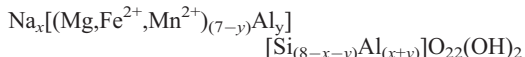
Spectroscopy

Site populations have been derived for orthorhombic amphiboles by both Mössbauer and infrared (IR) spectroscopies. Strens (1966, 1974), Bancroft *et al.* (1966), Burns and Law (1970), Fabriès and Perseil (1971), Law (1976, 1981), Ishida (1998) and Ishida and Hawthorne (2003) have reported IR spectra of orthorhombic amphiboles of the anthophyllite–gedrite series, in some cases deriving site populations from the band intensities in the principal OH-stretching region. Mössbauer spectra for these amphiboles have been reported by Bancroft *et al.* (1966, 1967), Bancroft and Burns (1968), Barabanov and Tomilov (1973), Seifert and Virgo (1974), Seifert (1977, 1978) and Stroink *et al.* (1980) and site populations were derived. Electronic absorption spectra were reported for anthophyllite and gedrite by Mao and Seifert (1974).

Chemical composition

The stoichiometry of the anthophyllite–gedrite series was established in the course of many studies following solution of the crystal structure of anthophyllite by Warren and Modell (1930).

Rabbitt (1948) reviewed all previous work and noted that orthorhombic amphibole has been the subject of study by most of the better known mineralogists and petrologists of the times. He described the series as varying from $Mg_7Si_8O_{22}(OH)_2$ to $Mg_5Al_2Si_6Al_2O_{22}(OH)_2$, and recommended that the term gedrite be dropped and replaced by “aluminian anthophyllite”. Robinson and Jaffe (1969) and Robinson *et al.* (1971) showed that Na is an essential constituent of the gedritic amphiboles, and formulated the currently accepted form for the general composition of gedrite. Berg (1985) showed that Na may reach close to 1 a.p.f.u. (atom per formula unit), completely filling the *A* site. Robinson and Jaffe (1969) and Ross *et al.* (1969) found that amphiboles intermediate in composition between anthophyllite and gedrite are unmixed at the microscopic or submicroscopic scale along lamellae parallel to (010). Stout (1971) confirmed the presence of a solvus by finding coarse coexisting orthorhombic amphiboles. Spear (1980) used natural samples to propose an asymmetrical solvus with a critical temperature of $\sim 600^\circ\text{C}$, expanding in width toward more Fe-rich compositions. The occurrence of a solvus was supported by the microstructural observations of Gittos *et al.* (1976), Treloar and Putnis (1982), Smelik and Veblen (1993), Champness and Rodgers (2000) and Müller *et al.* (2003). Leake *et al.* (1997) gave the (Li-free) formula of the orthorhombic amphiboles as



where $0.0 < x < 1.0$ and $0.00 < y < 2.0$ a.p.f.u.

Natural gedrite encompasses virtually the entire possible range of Fe–Mg solid solution, from at least 6% to 100% of the Fe end-member (Fabriès and Perseil, 1971; Robinson *et al.*, 1981). Substitution of Fe in natural anthophyllite, however, is limited to less (usually much less) than ~47% of the Fe end-member, its place being gradually taken over by cummingtonite–grunerite. An azeotropic relation between the two enables possible stable Fe-anthophyllite to surface at the end-member composition (Evans *et al.*, 2001).

Gedrite occurs principally in low-Ca amphibolites, low-K metapelites, metagabbros, and high-Mg–Al rocks formed by diffusive reaction at contacts with ultramafic rock. Associated minerals reflect these kinds of composition: Ca-amphibole, orthopyroxene, plagioclase, biotite,

garnet, cordierite, staurolite, the aluminosilicates, corundum, sapphirine and rutile. Igneous gedrite has recently been reported (Claeson and Meurer, 2002). In contrast, low-Al anthophyllite occurs predominantly in metaperidotite.

Experimental methods

The provenance of samples used in this work is shown in Table 1. The twenty-five amphibole samples (eleven of them heat-treated according to the procedure of Hirschmann *et al.*, 1994) cover most of the anthophyllite–gedrite solid-solution series and are primarily from amphibolite-facies metamorphic rocks. Many of the samples have been studied previously, and detailed descriptions can be found in the references cited in Table 1.

TABLE 1. Sample numbers and provenance for the samples used in this work.

Sample no.	Unheated	Heated*	Original sample no.	Provenance	Ref.
NMNH 103148-4	A1	A14	89	Shuyaratskaya, Karelia, Russia	—
NMNH 105352	A2	A19	84	Cherry Creek, Madison Co., Montana (Rabbit #1)	(1)
NMNH 138342	A3	A21	87	Guidres, France	
NMNH 146173	A4***	A17	92	Haddam, Connecticut	
NHM 93327	A5	A18	93		
NMNH 105354	A6	A12, A8	86	Dillon, Montana (Rabbit #9)	(1)
I34I**	A7, A9			Amphibole Hill area, New Hampshire	(2),(3), (4),(5)
Q544-P	A10	A16	91	North-central Massachusetts	(6)
OR26A		A11	77	Orijärvi, Finland	(7)
UBC 20257 (was M337E2)		A13	88	Falun, Norway	
W95S	A20	A15	90	Amphibole Hill area, New Hampshire	(6)
AMNH 166389	A22			Greenland	
N30X-1	A23			Amphibole Hill area, New Hampshire	(2),(4)
6A9X	A24			Amphibole Hill area, New Hampshire	(2),(4)
NHM 1936	A25			Kongsberg, Norway	
AMNH 136484	A26			North Carolina	

References: (1) Rabbitt (1948); (2) Robinson and Jaffe (1969); (3) Papike and Ross (1970); (4) Robinson *et al.* (1971); (5) Law (1982, 1989); (6) Schumacher and Robinson (1987); (7) Schneidermann and Tracy (1991).

* Hydrothermally treated for 4 days at 700°C, 2 kbar on the C–CH₄ buffer.

** Collected by BWE.

*** Could not be refined adequately.

NMNH: National Museum of Natural History, Washington, D.C.: AMNH: American Museum of Natural History, New York; NHM: Natural History Museum, London; UBC: University of British Columbia, Vancouver, BC.

Collection of X-ray data

Crystals used for the collection of single-crystal X-ray diffraction (XRD) data were mounted on a Siemens *P4* diffractometer fitted with a CCD detector and using Mo- $K\alpha$ X-radiation. For each crystal, integrated intensities were collected for the whole sphere of reciprocal space using 30 s per frame. Unit-cell parameters were refined from ~4000 reflections with ($I > 10 \sigma I$). An empirical absorption correction (SADABS; Sheldrick, 1998) was applied. Details of data collection and refined unit-cell parameters are given in Table 2.

Mössbauer spectroscopy

Mössbauer spectroscopy measurements were done in transmission geometry at room temperature (RT) using a $^{57}\text{Co}(\text{Rh})$ point source. The spectrometer was calibrated with the RT spectrum of α -Fe. For preparing the Mössbauer absorber, powdered amphibole was mixed with sugar and

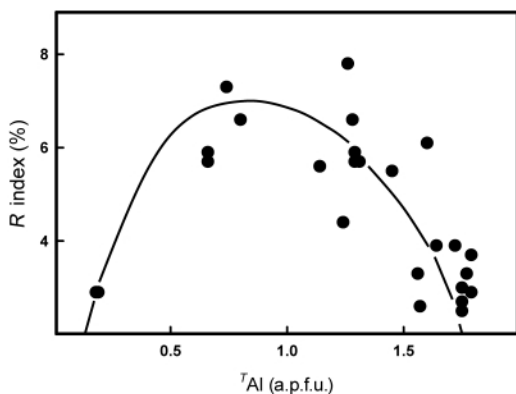


FIG. 2. Variation in R_1 index with $[^{41}\text{Al}]$ content in the orthorhombic amphiboles of this work; the line is drawn as a guide to the eye.

finely ground under acetone to avoid oxidation. The mixture was then loaded into a Pb ring (2 mm inner diameter) and covered by tape on both sides.

TABLE 2. Miscellaneous information for orthorhombic amphiboles.

	a (Δ)	b (Δ)	c (Δ)	V (Δ^3)	N ($>4\sigma$)	R (%)	Dimensions (mm)
A(1)	18.5553(5)	17.8275(5)	5.2795(1)	1746.4(1)	1804	2.6	$0.10 \times 0.10 \times 0.03$
A(2)	18.5804(6)	17.8347(6)	5.2819(2)	1750.3(2)	1711	2.5	$0.03 \times 0.06 \times 0.02$
A(3)	18.586(1)	17.907(1)	5.2892(3)	1760.3(2)	1379	5.5	$0.09 \times 0.07 \times 0.03$
A(5)	18.5711(6)	18.0256(6)	5.2885(2)	1770.4(1)	1794	2.9	$0.19 \times 0.06 \times 0.06$
A(6)	18.565(1)	17.900(1)	5.2881(3)	1757.3(3)	1562	6.6	$0.10 \times 0.04 \times 0.03$
A(7)	18.5998(9)	17.8477(9)	5.2853(2)	1754.5(2)	1459	2.9	$0.09 \times 0.04 \times 0.04$
A(8)	18.553(1)	17.903(1)	5.2894(3)	1756.9(2)	1530	5.9	$0.10 \times 0.09 \times 0.02$
A(9)	18.602(2)	17.838(2)	5.2863(5)	1754.1(5)	1140	3.7	$0.07 \times 0.04 \times 0.03$
A(10)	18.5988(8)	17.8611(9)	5.2873(3)	1756.4(2)	1488	2.7	$0.20 \times 0.05 \times 0.03$
A(11)	18.618(2)	17.945(2)	5.3033(4)	1772.0(5)	790	6.1	$0.08 \times 0.05 \times 0.01$
A(12)	18.547(1)	17.910(1)	5.2929(3)	1758.2(3)	1580	5.7	$0.09 \times 0.06 \times 0.03$
A(13)	18.525(1)	17.8198(9)	5.2637(2)	1737.6(3)	1105	4.4	$0.06 \times 0.06 \times 0.02$
A(14)	18.5539(8)	17.8442(2)	5.2813(2)	1748.5(2)	1295	3.3	$0.10 \times 0.06 \times 0.02$
A(15)	18.568(1)	17.882(1)	5.2818(4)	1753.7(3)	1319	5.6	$0.06 \times 0.06 \times 0.01$
A(16)	18.613(1)	17.875(1)	5.2890(3)	1759.6(3)	1247	3.0	$0.08 \times 0.06 \times 0.02$
A(17)	18.620(1)	17.971(1)	5.2931(3)	1771.1(3)	1617	7.8	$0.21 \times 0.06 \times 0.02$
A(18)	18.5716(9)	18.0307(8)	5.2903(2)	1771.5(1)	1401	2.9	$0.20 \times 0.06 \times 0.02$
A(19)	18.5812(9)	17.8483(9)	5.2859(2)	1753.0(2)	1336	3.3	$0.09 \times 0.06 \times 0.02$
A(20)	18.5603(9)	17.840(1)	5.2778(3)	1747.6(2)	1751	5.7	$0.17 \times 0.06 \times 0.04$
A(21)	18.559(1)	17.900(1)	5.2930(1)	1758.3(3)	1076	3.9	$0.16 \times 0.04 \times 0.01$
A(22)	18.572(1)	17.996(1)	5.2883(3)	1767.4(3)	1674	7.3	$0.14 \times 0.05 \times 0.04$
A(23)	18.583(1)	18.016(1)	5.2900(3)	1771.1(2)	1753	5.7	$0.17 \times 0.04 \times 0.03$
A(24)	18.602(1)	18.034(1)	5.2963(2)	1776.8(2)	1698	5.9	$0.18 \times 0.05 \times 0.03$
A(25)	18.574(2)	17.947(1)	5.2819(4)	1760.7(4)	1373	6.6	$0.12 \times 0.06 \times 0.03$
A(26)	18.550(1)	17.806(1)	5.2734(2)	1741.8(2)	1581	3.9	$0.10 \times 0.05 \times 0.04$

Assuming a recoilless fraction of 0.7 for the Mössbauer absorber, the amounts of sample used corresponded to an absorber thickness of $\sim 2.5\text{--}5.0\text{ mg Fe/cm}^2$.

Electron-microprobe analysis (EMPA)

The chemical compositions of 25 single crystals used for collection of the X-ray intensity data

were determined by EMPA (10 points per crystal) using a Cameca SX50 operating in wavelength-dispersive spectroscopy (WDS) mode at 15 kV and 20 nA, 10 μm beam. The following standards were used: F-bearing riebeckite (F), albite (Na), olivine (Mg), scapolite (Si, Al), apatite (P), anhydrite (S), tugtupite (Cl), sanidine (K), anorthite (Ca), titanite (Ti), spessartine (Mn), fayalite (Fe), SrTiO_3 (Sr) and barite (Ba). Data

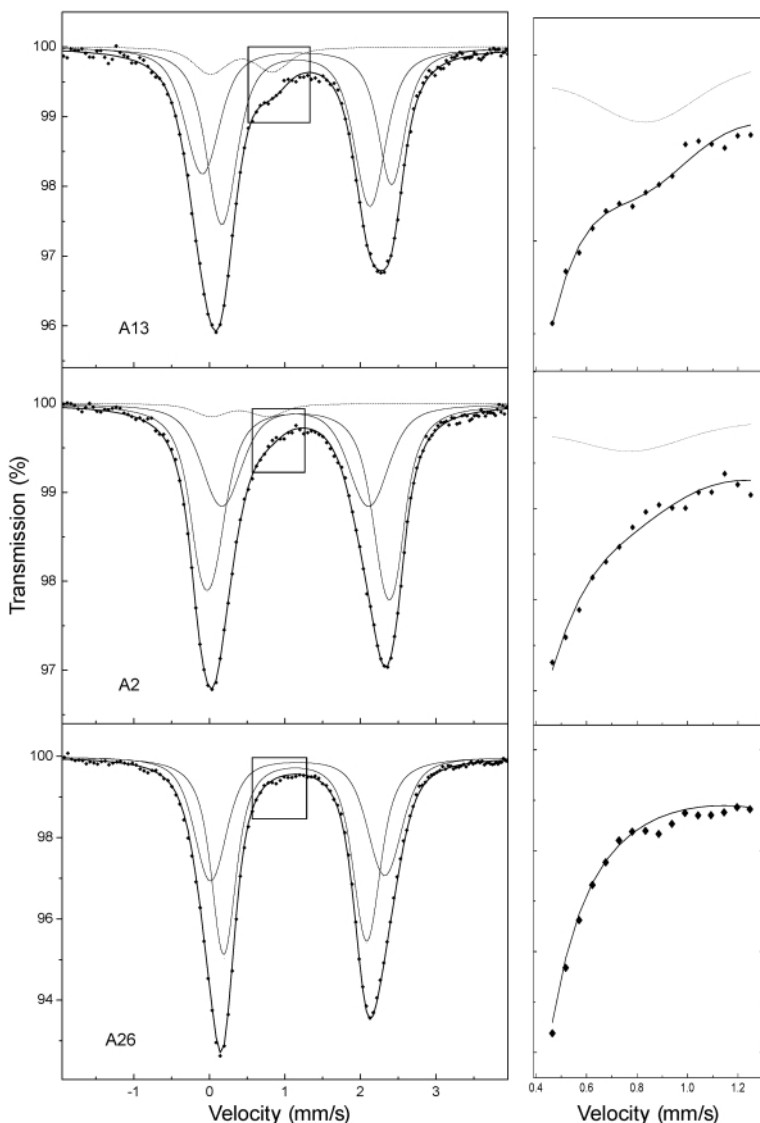


FIG. 3. Mössbauer spectra of selected orthorhombic amphiboles; on the left are spectra with maximum, intermediate and minimum (zero) amounts of Fe^{3+} ; on the right are enlarged views of part of the spectra around the high-velocity peak of the Fe^{3+} doublet.

TABLE 3. Chemical composition (wt.%) and unit formula (a.p.f.u.) of the anthophyllite–gedrite crystals of this work.

	A(1)	A(2)	A(3)	A(5)	A(6)	A(7)	A(8)	A(9)	A(10)	A(11)	A(12)	A(13)
SiO ₂	45.02	42.82	44.00	56.18	46.53	42.24	46.59	42.72	42.84	43.05	46.70	50.66
Al ₂ O ₃	16.24	17.68	14.20	2.32	12.54	17.65	12.59	17.68	16.95	15.10	12.70	13.31
TiO ₂	0.13	0.23	0.17	0.07	0.36	0.21	0.33	0.24	0.18	0.27	0.39	0.14
Fe ₂ O ₃	0.72	0.84	0.81	0.00	1.20	1.70	1.03	1.75	1.81	1.77	1.02	0.23
FeO	15.45	18.19	23.69	14.23	16.97	17.54	17.72	18.11	18.78	24.91	17.48	2.40
MnO	0.00	0.08	0.20	0.42	0.06	0.27	0.06	0.27	0.47	0.39	0.06	0.00
MgO	18.04	15.10	12.69	23.96	17.85	15.05	17.81	15.18	14.88	11.43	17.71	29.31
CaO	0.10	0.12	0.09	0.62	0.32	0.23	0.31	0.23	0.24	0.18	0.33	0.14
Na ₂ O	1.60	1.90	1.31	0.16	0.97	1.74	0.96	1.72	1.84	1.30	0.97	1.39
F	0.42	0.22	0.07	0.00	0.03	0.04	0.05	0.07	0.16	0.09	0.02	0.13
H ₂ O*	1.90	1.95	1.98	2.16	2.06	2.03	2.07	2.03	1.98	1.97	2.07	2.19
O=F	-0.18	-0.09	-0.03	0.00	-0.01	-0.02	-0.02	-0.03	-0.07	-0.04	-0.01	-0.05
Total	99.45	99.14	99.18	100.12	98.88	98.68	99.49	99.99	100.07	100.43	99.45	99.84
Si	6.42	6.23	6.55	7.81	6.72	6.18	6.71	6.18	6.23	6.39	6.72	6.75
Al	1.58	1.77	1.45	0.19	1.28	1.82	1.29	1.81	1.77	1.61	1.28	1.25
ΣT	8.00	8.00	8.00	8.00	8.00	8.00	8.00	8.00	8.00	8.00	8.00	8.00
Al	1.14	1.26	1.04	0.19	0.85	1.22	0.85	1.21	1.13	1.03	0.87	0.84
Ti ⁴⁺	0.01	0.03	0.02	0.01	0.04	0.02	0.03	0.03	0.02	0.03	0.04	0.01
Fe ³⁺	0.08	0.09	0.09	0.00	0.13	0.19	0.11	0.19	0.20	0.20	0.11	0.02
Fe ²⁺	1.84	2.21	2.95	1.66	2.05	2.15	2.13	2.19	2.28	3.09	2.10	0.27
Mg	3.84	3.30	2.82	4.97	3.85	3.30	3.83	3.29	3.24	2.54	3.80	5.83
Mn	0.00	0.01	0.03	0.05	0.01	0.03	0.01	0.03	0.06	0.05	0.01	0.00
Ca	0.02	0.02	0.01	0.09	0.05	0.04	0.05	0.04	0.04	0.03	0.05	0.02
ΣM	6.93	6.93	6.97	6.97	6.99	6.95	7.01	6.99	6.95	7.02	6.98	6.99
Na	0.44	0.54	0.38	0.04	0.27	0.50	0.27	0.49	0.52	0.38	0.27	0.36
F	0.19	0.10	0.03	0.00	0.01	0.02	0.02	0.03	0.07	0.04	0.01	0.06
OH	1.81	1.90	1.97	2.00	1.99	1.98	1.98	1.97	1.93	1.96	1.99	1.94

Calculated as OH = 2 - F a.p.f.u.

were reduced using the ZAF correction (PUMA program). FeO and Fe₂O₃ contents were calculated from the Fe³⁺/(Fe²⁺ + Fe³⁺) values derived from Mössbauer spectroscopy and the FeO values (treating all Fe as FeO) from EMPA. Unit formulae were calculated by normalizing on 24 anions assuming (OH) + F = 2 a.p.f.u. The final chemical compositions and unit formulae are given in Table 3.

Crystal-structure refinement

The structures of all crystals were refined with the *SHELXTL 5.1* software (Sheldrick, 1997). Scattering factors for neutral metal atoms were taken from the *International Tables for X-ray Crystallography* (Ibers and Hamilton, 1992); ionized scattering curves were used for O²⁻ and

Cl⁻. Refinement was initiated using the atom coordinates for anthophyllite (Finger, 1970) or gedrite (Papike and Ross, 1970). The occupancies of the *T*-sites cannot be refined because of the very small difference in X-ray scattering between Si (*Z* = 14) and Al (*Z* = 13). Based on the EMPA data and the <T-O> bond-lengths derived from the primary refinement, Si and Al occupancies were assigned to each tetrahedral site and fixed during subsequent stages of refinement. The *M* sites are occupied by Fe²⁺, Mg, Al, Fe³⁺ and minor Mn²⁺ and Ca; these scattering species were combined as Fe* (= Fe²⁺ + Fe³⁺ + Mn) and Mg* (= Mg + Al) and represented by the scattering curves for Fe and Mg. The *A* site is occupied by Na and □ (vacancy). Site occupancies of the *M* and *A* sites were considered as variable in the refinement. Full-matrix refinement of all variables

TABLE 3 (contd.).

	A(14)	A(15)	A(16)	A(17)	A(18)	A(19)	A(20)	A(21)	A(22)	A(23)	A(24)	A(25)	A(26)
SiO ₂	45.26	48.78	42.62	46.46	56.30	42.96	48.09	42.88	50.34	51.56	50.99	52.54	45.25
Al ₂ O ₃	15.98	12.01	17.14	10.55	2.25	18.10	13.90	14.96	7.38	6.45	6.50	8.56	17.74
TiO ₂	0.08	0.27	0.18	0.16	0.05	0.31	0.31	0.17	0.11	0.19	0.31	0.18	0.52
Fe ₂ O ₃	0.54	0.40	1.33	1.32	0.00	0.87	0.00	1.05	0.82	0.52	0.63	0.43	0.00
FeO	15.84	11.71	18.81	18.57	14.03	18.74	12.18	22.61	17.61	15.21	18.34	9.27	9.90
MnO	0.00	0.21	0.44	0.23	0.40	0.10	0.19	0.21	0.02	0.38	0.75	0.08	0.16
MgO	18.22	21.70	14.51	18.00	23.94	14.67	21.27	13.65	19.63	21.40	18.54	25.13	21.86
CaO	0.16	0.54	0.26	0.45	0.66	0.11	0.55	0.10	0.28	0.52	0.57	0.83	0.25
Na ₂ O	1.69	1.25	1.95	1.42	0.17	1.81	1.33	1.13	0.79	0.65	0.81	0.80	1.86
F	0.41	0.28	0.11	0.20	0.00	0.06	0.09	0.18	0.23	0.05	0.08	0.07	0.17
H ₂ O*	1.91	2.00	1.99	1.95	2.15	2.04	2.11	1.92	1.97	2.08	2.04	2.15	2.08
O=F	-0.17	-0.12	-0.05	-0.08	-0.00	-0.03	-0.04	-0.08	-0.10	-0.02	-0.03	-0.03	-0.07
Total	99.92	99.03	99.30	99.24	99.95	99.75	99.98	98.79	99.09	98.99	99.53	100.02	99.72
Si ⁴⁺	6.44	6.85	6.24	6.78	7.83	6.22	6.70	6.39	7.24	7.34	7.35	7.20	6.28
Al ³⁺	1.56	1.15	1.76	1.22	0.17	1.78	1.30	1.61	0.76	0.66	0.65	0.80	1.72
ΣT	8.00	8.00	8.00	8.00	8.00	8.00	8.00	8.00	8.00	8.00	8.00	8.00	8.00
Al	1.12	0.84	1.20	0.59	0.20	1.31	0.98	1.02	0.49	0.42	0.45	0.58	1.18
Ti ⁴⁺	0.01	0.03	0.02	0.02	0.01	0.03	0.03	0.02	0.01	0.02	0.03	0.02	0.05
Fe ³⁺	0.06	0.04	0.15	0.15	0.00	0.10	0.00	0.12	0.09	0.06	0.07	0.04	0.00
Fe ²⁺	1.88	1.38	2.30	2.27	1.63	2.27	1.42	2.82	2.12	1.81	2.21	1.06	1.15
Mg	3.86	4.55	3.18	3.92	4.97	3.17	4.41	3.02	4.22	4.54	3.98	5.14	4.52
Mn	0.00	0.03	0.06	0.03	0.05	0.01	0.02	0.03	0.00	0.05	0.09	0.01	0.02
Ca	0.02	0.08	0.04	0.07	0.10	0.02	0.08	0.02	0.04	0.08	0.09	0.12	0.04
ΣM	6.96	6.95	6.96	7.04	6.96	6.91	6.95	7.05	6.97	6.98	6.92	6.98	6.96
Na	0.47	0.34	0.56	0.40	0.05	0.51	0.36	0.33	0.22	0.18	0.23	0.21	0.50
F ⁻	0.19	0.12	0.05	0.09	0.00	0.03	0.04	0.09	0.11	0.02	0.04	0.03	0.08
OH ⁻	1.81	1.88	1.95	1.91	2.00	1.97	1.96	1.91	1.89	1.98	1.96	1.97	1.92

* Calculated as OH = 2 - F a.p.f.u.

for an anisotropic-displacement model converged to R_1 values in the range 2.5–7.8% with a mean value of 4.7%. Figure 2 shows the R_1 (%) index of each refinement as a function of the ⁷Al content of the crystal. The R_1 indices are small (<4%) at both ends of the series, but rise to a maximum of ~8% at intermediate compositions. Of course, there is much scatter in Fig. 2 as the coarseness of the exsolution lamellae will affect the diffraction, and this will vary from crystal to crystal, depending on their P - T histories. Nevertheless, Fig. 2 provides unmistakable evidence of the effect of exsolution on the quality of the structure refinement of crystals in this series. Final atom positions and equivalent-isotropic-displacement parameters are given in Table 4, selected interatomic distances and angles are listed in Table 5, and refined site-scattering values are given in Table 6.

Fitting of Mössbauer spectra

Figure 3 shows typical RT Mössbauer spectra for three anthophyllite–gedrite amphiboles. Most spectra were adequately fitted using a Voigt-based quadrupole-splitting distribution (QSD) method (Rancourt and Ping, 1991) for a model having three generalized sites, two for Fe²⁺ (A and B) and one for Fe³⁺, with one Gaussian component for each site. We allowed the linewidth (Γ) of the symmetrical elemental doublets of the QSD to be an adjustable parameter, and the centre shift (CS) to be linearly correlated to the quadrupole splitting (QS). Selected Mössbauer hyperfine parameters are listed in Table 7. Following the site assignments summarized by Hawthorne (1983) for amphiboles of the anthophyllite–gedrite series, we assign the generalized site with the larger average QS [Fe²⁺(A)] to Fe²⁺ at the M_1 , M_2 and M_3 sites. In the spectra where

TABLE 4a. Atomic coordinates and displacement parameters for the anthophyllites and gedrites of this work [samples A(1)–A(9)].

	A(1)	A(2)	A(3)	A(5)	A(6)	A(7)	A(8)	A(9)
O1A	<i>x</i> –0.17947(8)	–0.1789(1)	–0.1797(3)	–0.1825(1)	–0.1801(3)	–0.1789(1)	–0.1796(3)	–0.1790(2)
	<i>y</i> –0.1595(1)	–0.1584(1)	–0.1591(3)	–0.1629(1)	–0.1601(3)	–0.1582(2)	–0.1606(3)	–0.1583(3)
	<i>z</i> –0.0347(3)	–0.0327(4)	–0.036(1)	–0.0566(3)	–0.043(1)	–0.0313(4)	–0.0431(9)	–0.0321(7)
O1B	<i>x</i> 0.06971(9)	0.0700(1)	0.0700(4)	0.0681(1)	0.0685(3)	0.0700(1)	0.0687(3)	0.0701(2)
	<i>y</i> 0.1587(1)	0.1574(1)	0.1574(4)	0.1630(1)	0.1593(3)	0.1576(2)	0.1600(3)	0.1579(3)
	<i>z</i> –0.2869(3)	–0.2882(3)	–0.286(1)	–0.2745(3)	–0.2808(9)	–0.2889(4)	–0.2799(8)	–0.2884(7)
O2A	<i>x</i> 0.18436(9)	0.18443(9)	0.1852(3)	0.1855(1)	0.1845(3)	0.1845(1)	0.1842(3)	0.1843(2)
	<i>y</i> 0.07448(9)	0.0736(1)	0.0736(4)	0.0777(1)	0.0750(3)	0.0734(2)	0.0747(3)	0.0735(2)
	<i>z</i> –0.4419(3)	–0.4415(4)	–0.439(1)	–0.4368(3)	–0.4368(9)	–0.4416(4)	–0.4384(9)	–0.4425(8)
O2B	<i>x</i> 0.06320(8)	0.06293(9)	0.0628(3)	0.0628(1)	0.0630(3)	0.0629(1)	0.0627(3)	0.0628(2)
	<i>y</i> 0.07460(9)	0.0738(1)	0.0738(4)	0.0774(1)	0.0755(3)	0.0735(2)	0.0749(3)	0.0739(2)
	<i>z</i> 0.1874(3)	0.1845(4)	0.188(1)	0.2163(3)	0.198(1)	0.1837(5)	0.2005(9)	0.1846(8)
O3A	<i>x</i> 0.1805(1)	0.1809(1)	0.1818(5)	0.1817(2)	0.1812(4)	0.1805(2)	0.1813(4)	0.1807(3)
	<i>y</i> $\frac{1}{4}$	$\frac{1}{4}$						
	<i>z</i> –0.4605(4)	–0.4619(5)	–0.459(1)	–0.4441(5)	–0.456(1)	–0.4626(6)	–0.455(1)	–0.463(1)
O3B	<i>x</i> 119(8)	138(9)	110(33)	107(9)	119(3)	118(12)	118(28)	143(22)
	<i>y</i> $\frac{3}{4}$	$\frac{3}{4}$						
	<i>z</i> –0.0703(1)	–0.0704(1)	–0.0705(5)	–0.0695(2)	–0.0698(4)	–0.07031	–0.0701(4)	–0.0703(3)
O4A	<i>x</i> 0.18666(9)	0.1864(1)	0.1868(3)	0.1868(1)	0.1862(3)	0.1863(1)	0.1864(3)	0.1865(2)
	<i>y</i> 0.0024(1)	0.0025(1)	0.0013(3)	–0.0014(1)	0.0017(3)	0.0028(2)	0.0018(3)	0.0028(2)
	<i>z</i> 0.0480(3)	0.0462(4)	0.051(1)	0.0718(3)	0.057(1)	0.0453(4)	0.0574(9)	0.0457(8)
O4B	<i>x</i> 0.06898(8)	0.06830(9)	0.0687(3)	0.0668(1)	0.0684(3)	0.0685(1)	0.0675(3)	0.0686(2)
	<i>y</i> –0.0045(1)	–0.0047(1)	–0.0050(4)	–0.0066(1)	–0.0056(3)	–0.0048(2)	–0.0055(3)	–0.0052(3)
	<i>z</i> –0.2963(3)	–0.2974(4)	–0.298(1)	–0.2912(3)	–0.292(1)	–0.2965(4)	–0.2937(9)	–0.2963(8)
<i>U</i>	141(6)	112(23)	113(6)	116(20)	121(18)	111(18)	118(15)	118(15)

GEDRITE CRYSTAL CHEMISTRY. 1. CRYSTAL STRUCTURE

TABLE 4a (contd.)

	A(1)	A(2)	A(3)	A(5)	A(6)	A(7)	A(8)	A(9)
O5A	x 0.19687(8)	0.19691(9)	0.1971(3)	0.1977(1)	0.1974(3)	0.1972(1)	0.1975(3)	0.1969(2)
	y -0.1111(1)	-0.1104(1)	-0.1127(4)	-0.1175(1)	-0.1128(3)	-0.1105(2)	-0.1122(3)	-0.1105(2)
	z 0.3217(3)	0.3213(4)	0.321(1)	0.3282(4)	0.325(1)	0.3201(5)	0.3254(9)	0.3203(8)
	U 149(6)	162(6)	102(2)*	109(6)	122(19)	134(9)	126(18)	136(14)
O5B	x 0.05407(9)	0.05430(9)	0.0536(4)	0.0512(1)	0.0533(3)	0.0543(1)	0.0534(3)	0.0542(2)
	y -0.1025(1)	-0.1016(1)	-0.1031(4)	-0.11112(1)	-0.1053(4)	-0.1018(2)	-0.1056(3)	-0.1017(3)
	z 0.0922(3)	0.0962(4)	0.090(1)	0.0588(4)	0.081(1)	0.0558(5)	0.079(1)	0.0947(8)
	U 177	153(6)	163(24)	115(6)	223(22)	149(9)	207(21)	159(15)
O6A	x 0.20279(8)	0.2034(1)	0.2024(3)	0.2007(1)	0.2025(3)	0.2033(1)	0.2026(3)	0.2032(2)
	y -0.3682(1)	-0.3678(1)	-0.3687(3)	-0.3698(1)	-0.3692(3)	-0.3677(2)	-0.3685(3)	-0.3681(2)
	z -0.1745(3)	-0.1740(4)	-0.179(1)	-0.1742(4)	-0.176(1)	-0.1748(5)	-0.1753(9)	-0.1739(8)
	U 163(5)	157(6)	104(16)*	113(6)	102(13)*	139(9)	122(18)	155(15)
O6B	x 0.04778(9)	0.0472(1)	0.0465(4)	0.0484(1)	0.0477(3)	0.0473(1)	0.0481(3)	0.0473(2)
	y -0.1448(1)	-0.1457(1)	-0.1451(4)	-0.1404(1)	-0.1441(3)	-0.1456(2)	-0.1434(3)	-0.1456(2)
	z -0.4116(3)	-0.4065(4)	-0.411(1)	-0.4471(4)	-0.424(1)	-0.4058(5)	-0.424(1)	-0.4069(8)
	U 207(6)	200(7)	189(25)	127(6)	210(16)*	177(9)	210(21)	177(16)
O7A	x 0.2039(1)	0.2049(1)	0.2044(5)	0.2030(2)	0.2025(5)	0.2048(2)	0.2021(5)	0.2047(3)
	y 3/4	3/4	3/4	3/4	3/4	3/4	3/4	3/4
	z 0.5190(4)	0.5169(5)	0.525(1)	0.5401(5)	0.528(1)	0.5182(6)	0.526(1)	0.518(1)
	U 161(8)	157(9)	119(33)	108(9)	205(32)	148(13)	223(30)	142(22)
O7B	x 0.0454(1)	0.0447(1)	0.0464(5)	0.0463(2)	0.0444(4)	0.0450(2)	0.0446(4)	0.0443(3)
	y 3/4	3/4	3/4	3/4	3/4	3/4	3/4	3/4
	z 0.2182(4)	0.2187(5)	0.217(2)	0.2215(5)	0.224(1)	0.2187(6)	0.223(1)	0.218(1)
	U 156(8)	144(9)	135(34)	105(9)	67(19)*	135(12)	78(18)*	151(22)
T1A	x 0.23169(4)	0.23208(4)	0.2323(2)	0.23074(5)	0.2316(1)	0.23223(5)	0.2312(1)	0.2321(1)
	y -0.16315(4)	-0.16283(4)	-0.1634(2)	-0.16532(4)	-0.1638(2)	-0.16290(7)	-0.1639(1)	-0.1631(1)
	z -0.4485(1)	-0.4494(2)	-0.4469(5)	-0.4354(1)	-0.4425(4)	-0.4501(2)	-0.4418(4)	-0.4496(3)
	U 92(2)	83(2)	68(9)	74(2)	75(8)	68(3)	72(7)	74(6)
T1B	x 0.01992(4)	0.01982(4)	0.0199(2)	0.01882(5)	0.0196(1)	0.01978(5)	0.0198(1)	0.0196(1)
	y -0.16451(4)	-0.16438(4)	-0.1648(2)	-0.16621(4)	-0.1651(1)	-0.16437(6)	-0.1652(1)	-0.1645(1)
	z 0.2975(1)	0.3001(2)	0.2973(5)	0.2775(1)	0.2899(4)	0.3006(2)	0.2889(4)	0.3000(3)
	U 91(2)	79(2)	76(9)	75(2)	74(7)	66(3)	72(7)	73(6)
T2A	x 0.222798(4)	0.222798(4)	0.22279(2)	0.222745(4)	0.22280(1)	0.22799(5)	0.22279(1)	0.22279(1)
	y -0.07630(4)	-0.07609(4)	-0.0768(2)	-0.07942(4)	-0.0771(1)	-0.07610(6)	-0.0772(1)	-0.0761(1)
	z 0.0513(2)	0.0519(1)	0.0529(5)	0.0618(1)	0.0571(4)	0.0513(2)	0.0572(4)	0.0512(3)
	U 99(2)	90(2)	71(9)	79(2)	78(8)	78(3)	76(7)	88(6)

$T2B$	x	0.02638(3)	0.02658(4)	0.0268(2)	0.02488(4)	0.0261(1)	0.02658(5)	0.0261(1)
	y	-0.07994(4)	-0.07980(4)	-0.0805(2)	-0.08190(4)	-0.0806(1)	-0.07982(6)	-0.0799(1)
	z	-0.1993(1)	-0.967(2)	-0.200(5)	-0.2211(1)	-0.2076(4)	-0.1966(2)	-0.1967(3)
	U	96(2)	84(2)	81(9)	79(2)	76(8)	72(3)	69(7)

TABLE 4a (contd.)

		A(1)	A(2)	A(3)	A(5)	A(6)	A(7)	A(8)	A(9)
$M1$	x	0.12417(3)	0.12420(4)	0.12421(1)	0.12484(5)	0.1247(1)	0.12428(5)	0.1247(1)	0.12440(9)
	y	0.16096(4)	0.16075(3)	0.1607(1)	0.16287(4)	0.1614(1)	0.16065(5)	0.1616(1)	0.16076(8)
	z	0.37371(1)	0.37221(1)	0.3761(4)	0.3904(1)	0.3788(4)	0.3719(2)	0.3800(4)	0.3720(3)
	U	106(2)	116(2)	104(7)	94(3)	107(7)	85(3)	105(6)	67(6)
$M2$	x	0.12470(4)	0.12459(4)	0.1247(2)	0.12490(5)	0.1249(1)	0.12460(6)	0.1248(1)	0.1247(1)
	y	0.07258(4)	0.07226(4)	0.0716(2)	0.07298(5)	0.0721(1)	0.07217(6)	0.0722(1)	0.0721(1)
	z	-0.1267(1)	-0.1283(3)	-0.1256(6)	-0.1100(2)	-0.1214(5)	-0.1291(2)	-0.1207(4)	-0.1287(3)
	U	78(2)	63(3)	83(9)	89(3)	85(8)	55(3)	78(7)	67(6)
$M3$	x	0.12435(5)	0.12420(5)	0.1244(2)	0.12546(7)	0.1247(2)	0.12424(6)	0.1251(2)	0.1244(1)
	y	$\frac{1}{4}$							
	z	-0.1264(2)	-0.1283(2)	-0.1264(6)	-0.1094(2)	-0.1235(6)	-0.1285(2)	-0.1212(5)	-0.1285(4)
	U	104(3)	89(3)	93(9)	82(4)	84(10)	91(4)	86(9)	82(7)
$M4$	x	0.11904(2)	0.11855(3)	0.11920(8)	0.12319(3)	0.12021(8)	0.11852(3)	0.12064(9)	0.11856(6)
	y	-0.01457(3)	-0.01504(3)	-0.01443(9)	-0.01055(2)	-0.01360(8)	-0.01520(4)	-0.01304(8)	-0.01513(6)
	z	0.36745(8)	0.36581(1)	0.3696(3)	0.38699(9)	0.3747(3)	0.3651(1)	0.3751(3)	0.3655(2)
	U	142(1)	128(2)	136(5)	122(1)	150(5)	117(2)	146(5)	123(4)
A	x	0.1148(2)	0.1162(2)	0.1164(8)	—	0.115(1)	0.1163(2)	0.115(1)	0.1173(5)
	y	$\frac{3}{4}$	$\frac{3}{4}$	$\frac{3}{4}$	—	$\frac{3}{4}$	$\frac{3}{4}$	$\frac{3}{4}$	$\frac{3}{4}$
	z	0.8400(8)	0.8453(8)	300	—	0.843(4)	0.8454(9)	0.851(4)	0.843(2)
U		300	—	—	300	300	300	300	300

GEDRITE CRYSTAL CHEMISTRY. 1. CRYSTAL STRUCTURE

TABLE 4b. Atomic coordinates and displacement parameters for the anthophyllites and gedrites of this work [samples A(10)–A(18)].

	A(10)	A(11)	A(12)	A(13)	A(14)	A(15)	A(16)	A(17)	A(18)
O1A	x y z	-0.1789(1) -0.1586(1) -0.0335(4)	-0.1806(7) -0.1591(9) -0.033(2)	-0.1798(3) -0.1606(3) -0.0440(9)	-0.1800(2) -0.1613(3) -0.0405(9)	-0.1806(3) -0.1615(4) -0.042(1)	-0.1791(2) -0.1593(2) -0.0331(5)	-0.1794(4) -0.1618(4) -0.046(1)	-0.1826(2) -0.1629(1) -0.0559(4)
	U	132(8)	160(46)*	145(14)*	114(24)	136(13)	145(25)	128(12)	143(19)*
									94(10)
O1B	x y z	0.0699(1) 0.1580(1) -0.2892(4)	0.0708(8) 0.1573(9) -0.283(2)	0.0688(3) 0.1598(3) -0.2792(8)	0.0694(3) 0.1610(3) -0.2827(9)	0.0693(3) 0.1602(4) -0.2800(9)	0.0702(2) 0.1587(2) -0.2875(5)	0.0672(4) 0.1606(4) -0.279(1)	0.0681(2) 0.1628(1) -0.2736(4)
	U	136(8)	148(46)*	92(12)*	113(24)	134(13)	109(23)	145(13)	99(17)*
									92(9)
O2A	x y z	0.1845(1) 0.0737(0) -0.4425(4)	0.1855(6) 0.0737(8) -0.4372(4)	0.1842(3) 0.0747(3) -0.4377(8)	0.1843(3) 0.0748(3) -0.4458(9)	0.1844(2) 0.0743(2) -0.4416(5)	0.1851(3) 0.0750(3) -0.440(1)	0.1839(4) 0.0736(2) -0.4438(5)	0.1856(2) 0.0751(4) -0.4379(4)
	U	134(8)	45(37)*	104(16)	105(21)	111(11)	97(20)	100(10)	106(16)*
									86(9)
O2B	x y z	0.0627(1) 0.0739(1) 0.1860(5)	0.0626(7) 0.0731(8) 0.190(2)	0.0626(3) 0.0747(3) 0.2004(8)	0.0631(3) 0.0744(3) 0.199(1)	0.0631(2) 0.0740(2) 0.1919(6)	0.0630(3) 0.0749(3) 0.200(1)	0.0627(2) 0.0754(2) 0.1883(6)	0.0616(4) 0.0756(4) 0.204(1)
	U	134(8)	169(42)*	115(16)	105(21)	133(11)	138(22)	132(11)	119(17)*
									112(9)
O3A	x y z	0.1805(2) $\frac{1}{4}$ -0.4620(6)	0.181(6) $\frac{1}{4}$ -0.455(3)	0.1812(4) $\frac{1}{4}$ -0.453(1)	0.1810(4) $\frac{1}{4}$ -0.455(1)	0.1803(3) $\frac{1}{4}$ -0.452(8)	0.1818(5) $\frac{1}{4}$ -0.452(2)	0.1806(3) $\frac{1}{4}$ -0.4587(8)	0.1803(6) $\frac{1}{4}$ -0.453(2)
	U	125(11)	149(7)*	134(25)	119(33)	116(17)	138(34)	141(17)	144(26)*
									118(15)
O3B	x y $\frac{3}{4}$	-0.0705(2) -0.071(1)	-0.071(1)	$\frac{3}{4}$	-0.0694(4) $\frac{3}{4}$	-0.0707(4) $\frac{3}{4}$	-0.0706(3) $\frac{3}{4}$	-0.0704(5) $\frac{3}{4}$	-0.0685(5) $\frac{3}{4}$
	U								-0.0693(2) $\frac{3}{4}$
									0.7738(7)
O4A	x y z	0.1866(1) 0.0023(1) 0.0466(4)	0.1875(7) 0.0016(8) 0.052(2)	0.1863(3) 0.0019(3) 0.0571(9)	0.1877(3) 0.0026(3) 0.052(1)	0.1869(2) 0.0027(2) 0.0496(6)	0.1877(3) 0.0023(3) 0.054(1)	0.1865(4) 0.0025(2) 0.0459(5)	0.1865(2) 0.0005(4) 0.0715(5)
	U	124(8)	118(41)*	129(17)	109(21)	128(12)	124(22)	117(11)	132(17)*
									108(9)
O4B	x y z	0.0682(1) -0.0049(1) -0.2969(5)	0.0687(7) -0.0048(8) -0.2962(2)	0.0680(3) -0.0052(3) -0.2934(8)	0.0679(3) -0.0063(3) -0.300(1)	0.0679(2) -0.0050(2) -0.2970(5)	0.0679(3) -0.0058(4) -0.295(1)	0.0682(2) -0.0054(2) -0.2975(6)	0.0675(4) -0.0062(4) -0.295(1)
	U	140(8)	85(41)*	114(17)	129(22)	131(12)	138(22)	130(12)	122(17)*
									111(9)
O5A	x y z	0.1972(1) -0.11110(1) 0.3220(5)	0.1966(7) -0.1116(7) 0.314(2)	0.1970(3) -0.11095(3) 0.3271(8)	0.1964(2) -0.1104(2) 0.330(1)	0.1967(2) -0.1118(4) 0.3242(6)	0.1971(3) -0.1100(2) 0.329(1)	0.1981(4) -0.1137(4) 0.3222(6)	0.1978(2) -0.1167(1) 0.3309(5)
	U	143(8)	69(34)*	139(17)					122(2)*
									104(9)

TABLE 4b (contd.)

	A(10)	A(11)	A(12)	A(13)	A(14)	A(15)	A(16)	A(17)	A(18)
O5B	x 0.0541(1)	0.0524(7)	0.0532(3)	0.0529(3)	0.0533(2)	0.0522(3)	0.0538(2)	0.0522(4)	0.0510(2)
	y -0.1021(1)	-0.1038(8)	-0.1056(3)	-0.1037(3)	-0.1033(2)	-0.1055(4)	-0.1025(2)	-0.1071(4)	-0.1117(2)
	z 0.0935(5)	0.091(2)	0.0779(9)	0.084(1)	0.0876(6)	0.079(1)	0.0908(6)	0.075(1)	0.0566(5)
O6A	U 154(8)	131(36)*	197(19)	167(21)	166(12)	209(25)	150(11)	221(19)*	118(9)
	x 0.2032(1)	0.2017(7)	0.2024(3)	0.2017(3)	0.2026(2)	0.2022(3)	0.2032(2)	0.2022(4)	0.2010(2)
	y -0.3681(1)	-0.3688(7)	-0.3683(3)	-0.3663(3)	-0.3676(2)	-0.3676(2)	-0.3676(2)	-0.3688(4)	-0.3692(1)
O6B	z -0.1745(5)	-0.182(2)	-0.1715(9)	-0.168(1)	-0.1736(6)	-0.172(1)	-0.1733(6)	-0.176(1)	-0.1733(5)
	U 149(8)	143(37)*	130(12)*	144(19)	147(12)	133(21)	152(11)	99(16)*	125(9)
	x 0.0473(1)	0.0449(6)	0.0477(3)	0.0478(3)	0.0471(2)	0.0472(3)	0.0472(2)	0.0478(4)	0.0481(1)
O7A	y -0.1454(1)	-0.1447(7)	-0.1434(3)	-0.1449(3)	-0.1447(2)	-0.1440(4)	-0.1454(2)	-0.1439(4)	-0.1403(1)
	z -0.4082(5)	-0.413(2)	-0.4257(9)	-0.418(1)	-0.4147(6)	-0.425(1)	-0.4090(6)	-0.425(1)	-0.4479(5)
	U 191(9)	97(35)*	197(19)	173(2)	183(13)	198(24)	198(12)	223(19)*	127(9)
O7B	x 0.2044(2)	0.206(1)	0.2028(4)	0.2019(4)	0.2031(3)	0.2034(4)	0.2036(3)	0.2017(6)	0.2021(2)
	y $\frac{3}{4}$	$\frac{3}{4}$							
	z 0.5177(6)	0.524(3)	0.524(1)	0.513(1)	0.5185(8)	0.519(2)	0.5181(7)	0.530(2)	0.5392(6)
T1A	U 150(12)	67(56)*	196(2)	182(33)	149(18)	217(3)	170(18)	208(28)*	100(13)
	x 0.0449(2)	0.047(1)	0.0452(4)	0.0463(4)	0.0460(3)	0.0458(4)	0.0457(3)	0.0448(5)	0.0461(2)
	y $\frac{3}{4}$	$\frac{3}{4}$							
T1B	z 0.2182(6)	0.221(3)	0.222(1)	0.218(1)	0.2185(8)	0.224(1)	0.2177(8)	0.223(2)	0.2223(6)
	U 144(12)	249(69)*	104(17)*	130(29)	135(17)	79(21)	153(17)	97(23)*	108(14)
	x 0.23208(5)	0.2323(4)	0.2312(1)	0.2307(1)	0.2314(8)	0.2313(1)	0.2319(8)	0.2318(2)	0.23050(7)
T2A	y -0.16298(5)	-0.1637(4)	-0.1639(1)	-0.1639(1)	-0.1633(8)	-0.1639(1)	-0.16305(8)	-0.1643(2)	-0.16536(6)
	z -0.4496(2)	-0.4478(9)	-0.4424(4)	-0.4447(4)	-0.4449(2)	-0.4432(5)	-0.4496(2)	-0.4406(5)	-0.4345(2)
	U 76(3)	73(23)	71(7)	74(8)	79(5)	73(9)	76(4)	73(9)	59(3)
T2B	x 0.01978(5)	0.0195(4)	0.0196(1)	0.0196(1)	0.0196(8)	0.0198(1)	0.01969(7)	0.0194(2)	0.01856(7)
	y -0.16462(5)	-0.1650(4)	-0.1651(1)	-0.1653(1)	-0.16479(8)	-0.1654(1)	-0.16466(8)	-0.1655(2)	-0.16621(6)
	z 0.2996(2)	0.2962(9)	0.2890(4)	0.2915(4)	0.2956(2)	0.2892(5)	0.2987(3)	0.2868(5)	0.2764(2)
T2A	U 76(3)	81(22)	78(6)	80(8)	79(5)	63(8)	72(7)	77(9)	51(4)
	x 0.22799(5)	0.2279(4)	0.2279(1)	0.2276(1)	0.22787(8)	0.2282(1)	0.22792(8)	0.2280(2)	0.22727(7)
	y -0.07627(5)	-0.0765(4)	-0.0771(1)	-0.0769(1)	-0.07635(8)	-0.0772(1)	-0.07622(8)	-0.0779(2)	-0.07937(6)
T2B	z 0.0509(2)	0.0529(9)	0.0572(4)	0.0548(4)	0.0534(2)	0.0550(5)	0.0513(2)	0.0585(5)	0.0623(2)
	U 86(3)	69(24)	81(7)	83(8)	82(5)	88(8)	82(4)	75(9)	80(4)

<i>T2B</i>	<i>x</i>	0.02652(5)	0.0271(4)	0.0261(1)	0.02632(8)	0.0262(1)	0.0265(1)	0.0259(2)	0.02472(7)
	<i>y</i>	-0.08005(5)	-0.0808(4)	-0.0801(1)	-0.07991(8)	-0.0804(1)	-0.0801(1)	-0.0811(2)	-0.08175(6)
	<i>z</i>	-0.1976(2)	-0.203(1)	-0.2082(4)	-0.2069(4)	-0.2025(3)	-0.2078(5)	-0.2117(5)	-0.22224(2)
	<i>U</i>	79(3)	80(24)	79(6)	67(7)	79(5)	74(8)	76(7)	60(4)

TABLE 4*b* (*contd.*)

	A(10)	A(11)	A(12)	A(13)	A(14)	A(15)	A(16)	A(17)	A(18)
<i>M1</i>	<i>x</i>	0.12429(4)	0.1245(3)	0.1248(1)	0.1248(2)	0.12438(8)	0.1247(1)	0.12441(6)	0.1249(2)
	<i>y</i>	0.16075(4)	0.1606(2)	0.16161(9)	0.1619(1)	0.16098(6)	0.1617(1)	0.16071(6)	0.1616(1)
	<i>z</i>	0.3725(2)	0.3769(8)	0.3794(3)	0.3767(6)	0.3754(2)	0.3778(5)	0.3731(2)	0.3821(4)
<i>M2</i>	<i>U</i>	104(3)	110(15)	104(5)	131(10)	115(4)	101(8)	109(3)	96(7)
	<i>x</i>	0.12456(5)	0.1248(4)	0.1248(1)	0.1247(2)	0.12469(8)	0.1247(1)	0.12460(7)	0.1248(2)
	<i>y</i>	0.07224(5)	0.0716(3)	0.0721(1)	0.0727(1)	0.07240(7)	0.0724(1)	0.07218(7)	0.0720(1)
<i>M3</i>	<i>z</i>	-0.1282(2)	-0.124(1)	-0.1212(4)	-0.1269(5)	-0.1261(3)	-0.1235(5)	-0.1285(2)	-0.1189(5)
	<i>U</i>	69(3)	92(20)	78(6)	61(9)	78(4)	68(9)	76(4)	104(8)
	<i>x</i>	0.12425(6)	0.1248(4)	0.1252(2)	0.1254(2)	0.1248(1)	0.1252(2)	0.12457(9)	0.1251(2)
<i>M4</i>	<i>y</i>	$\frac{1}{4}$							
	<i>z</i>	-0.1278(2)	-0.124(1)	-0.1211(5)	-0.1235(8)	-0.1253(3)	-0.1229(8)	-0.1271(3)	-0.1194(6)
	<i>U</i>	87(4)	90(2)	90(8)	65(13)	91(6)	76(12)	97(5)	103(11)
<i>A</i>	<i>x</i>	0.11869(3)	0.1197(2)	0.12066(8)	0.1217(2)	0.1198(6)	0.1211(1)	0.11933(5)	0.1215(1)
	<i>y</i>	-0.01513(3)	-0.0143(2)	-0.01320(8)	-0.0115(1)	-0.01391(5)	-0.0128(1)	-0.01476(5)	-0.0123(1)
	<i>z</i>	0.3659(1)	0.3721(7)	0.3745(3)	0.3678(6)	0.3686(2)	0.3721(4)	0.3657(2)	0.3768(3)
<i>A</i>	<i>U</i>	126(2)	147(12)	152(5)	179(10)	140(3)	148(7)	132(3)	160(6)
	<i>x</i>	0.1161(2)	0.117(1)	0.115(1)	0.1164(8)	0.1151(5)	0.1165(9)	0.1166(3)	0.116(1)
	<i>y</i>	$\frac{3}{4}$	$\frac{3}{4}$	$\frac{3}{4}$	$\frac{3}{4}$	0.841(1)	$\frac{3}{4}$	$\frac{3}{4}$	0.843(3)
<i>A</i>	<i>z</i>	0.8445(9)	0.838(5)	0.841(3)	0.839(3)	300	300	300	300
	<i>U</i>	300							300

TABLE 4c. Atomic coordinates and displacement parameters for the anthophyllites and gedrites of this work [samples A(19)–A(26)].

	A(19)	A(20)	A(21)	A(22)	A(23)	A(24)	A(25)	A(26)
O1A	x –0.1791(2) y –0.1592(2) z –0.0326(5)	–0.1802(2) –0.1603(3) –0.0374(8)	–0.1797(2) –0.1590(3) –0.0358(8)	–0.1814(3) –0.1622(3) –0.0527(10)	0.1816(2) 0.1623(20) 0.0522(7)	0.1814(2) 0.1622(2) 0.0524(8)	0.17915(11) 0.15972(13) 0.0323(4)	0.17915(11) 0.15972(13) 0.0323(4)
O1B	x 0.0700(2) y 0.1580(2) z –0.2875(6)	0.0696(2) 0.1600(3) –0.2868(8)	0.0699(2) 0.1583(3) –0.2825(8)	0.0687(3) 0.1618(3) –0.2776(9)	0.0688(20) 0.16228(20) –0.2777(7)	0.0687(2) 0.1621(2) –0.2769(7)	0.06998(12) 0.15890(12) –0.2795(8)	0.06998(12) 0.15890(12) –0.2795(8)
O2A	x 0.1844(2) y 0.0733(2) z –0.4416(6)	0.1846(2) 0.0750(3) –0.4441(8)	0.1845(2) 0.0736(2) –0.4380(8)	0.1856(3) 0.0764(3) –0.4559(9)	0.18544(20) 0.07640(20) –0.4381(7)	0.1856(2) 0.0758(2) –0.4384(7)	0.1843(2) 0.0764(2) –0.4387(8)	0.1843(2) 0.07394(12) –0.4459(4)
O2B	x 0.0625(2) y 0.0732(2) z 0.1863(6)	0.0633(2) 0.0750(3) 0.1935(8)	0.0629(2) 0.0734(3) 0.1909(9)	0.0628(3) 0.0765(3) 0.2087(10)	0.06296(19) 0.07593(20) 0.2116(7)	0.0628(2) 0.0760(2) 0.2114(8)	0.0631(2) 0.0760(2) 0.2076(8)	0.06304(11) 0.0764(11) 0.1864(4)
O3A	x 0.1808(2) y $\frac{1}{4}$ z –0.4604(8)	0.1813(4) $\frac{1}{4}$ –0.4591(1) 110(22)	0.1811(4) $\frac{1}{4}$ –0.4551(1) 115(19)*	0.1815(4) $\frac{1}{4}$ –0.4459(13) 113(15)	0.1820(3) $\frac{1}{4}$ –0.4463(10) 151(12)	0.1819(4) $\frac{1}{4}$ –0.4458(11) 128(13)	0.1824(4) $\frac{1}{4}$ –0.4490(12) 144(15)	0.1810(17) $\frac{1}{4}$ –0.4617(6) 110(7)
O3B	x –0.0704(2) y $\frac{3}{4}$ z 0.7892(8)	–0.0706(4) $\frac{3}{4}$ –0.4591(1) 129(23)	–0.0702(4) $\frac{3}{4}$ –0.4551(1) 145(26)	–0.0693(4) $\frac{3}{4}$ –0.4459(13) 94(14)	–0.0694(3) $\frac{3}{4}$ –0.4463(10) 103(10)	–0.0692(3) $\frac{3}{4}$ –0.4458(11) 105(12)	–0.0685(3) $\frac{3}{4}$ –0.4490(12) 75(13)	–0.07002(16) $\frac{3}{4}$ –0.4617(6) 107(7)
O4A	x 0.1865(2) y 0.0028(2) z 0.0466(6)	0.1869(2) 0.0021(3) 0.0525(9)	0.1859(2) 0.0022(2) 0.0482(8)	0.1863(3) –0.0010(3) 0.0700(11)	0.18673(20) –0.0007(2) 0.0670(8)	0.1867(2) –0.0010(3) 0.0677(8)	0.1870(3) 0.0005(2) 0.0610(8)	0.18664(11) 0.00308(12) 0.0437(4)
O4B	x 0.0683(2) y –0.0049(2) z –0.2976(6)	0.0680(2) –0.0052(3) –0.2945(8)	0.0685(2) –0.0049(3) –0.2945(8)	0.0673(3) –0.0062(3) –0.2925(10)	0.06753(20) –0.00648(20) –0.2936(7)	0.0671(2) –0.00642(2) –0.2920(8)	0.06821(11) –0.00602(2) –0.2934(8)	0.06821(11) –0.00479(12) –0.2987(4)
	U 127(11) U 135(11) U 135(11) U 113(10) U 113(10) U 120(1) U 120(1) U 125(16) U 125(16)	100(17) 143(16) 100(17) 143(16)	114(11) 134(8) 100(17) 143(16)		114(9) 110(10) 122(5) 119(10) 109(5)		134(8) 124(10)	134(5)

O5A	<i>x</i>	0.1965(2)	0.1971(2)	0.1970(2)	0.1975(3)	0.19727(20)	0.1975(2)	0.19680(11)
	<i>y</i>	-0.1096(2)	-0.1120(3)	-0.1117(3)	-0.1158(3)	-0.1152(2)	-0.1160(2)	-0.110952(13)
	<i>z</i>	0.3223(6)	0.3218(8)	0.3216(9)	0.3281(10)	0.3300(7)	0.3273(8)	0.3284(8)
	<i>U</i>	116(10)	149(16)	117(16)	133(11)	153(8)	147(9)	139(10)

TABLE 4c (*contd.*)

	A(19)	A(20)	A(21)	A(22)	A(23)	A(24)	A(25)	A(26)
O5B	<i>x</i>	0.0540(2)	0.0533(3)	0.0539(2)	0.0517(3)	0.05117(20)	0.0514(2)	0.0518(2)
	<i>y</i>	-0.1020(2)	-0.1038(3)	-0.1033(3)	-0.1101(3)	-0.1098(2)	-0.1104(3)	-0.1081(3)
	<i>z</i>	0.0920(6)	0.0891(9)	0.0861(9)	0.0662(11)	0.06534(8)	0.0629(8)	0.0711(8)
	<i>U</i>	139(11)	195(17)	143(17)	188(13)	166(9)	173(10)	184(11)
O6A	<i>x</i>	0.2031(2)	0.2025(2)	0.2030(2)	0.2015(3)	0.2015(2)	0.2014(2)	0.2015(3)
	<i>y</i>	-0.3674(2)	-0.3682(3)	-0.3685(2)	-0.1304(3)	-0.1310(2)	-0.1306(3)	-0.1313(3)
	<i>z</i>	-0.1729(6)	-0.1779(8)	-0.1749(9)	-0.1718(10)	-0.1718(7)	-0.1723(8)	-0.1737(8)
	<i>U</i>	148(11)	111(11)	145(16)	146(11)	157(8)	147(10)	159(10)
O6B	<i>x</i>	0.0469(2)	0.0475(3)	0.0471(2)	0.0483(3)	0.0478(2)	0.0484(2)	0.0483(2)
	<i>y</i>	-0.1452(2)	-0.1449(3)	-0.1437(2)	-0.144(4)	-0.1412(2)	-0.1408(3)	-0.1426(3)
	<i>z</i>	-0.4085(6)	-0.4137(9)	-0.4171(9)	-0.4405(11)	-0.4411(8)	-0.4420(9)	-0.4351(8)
	<i>U</i>	179(12)	225(18)	175(18)	195(13)	190(9)	193(10)	183(11)
O7A	<i>x</i>	0.2038(3)	0.2026(4)	0.2041(4)	0.2037(4)	0.2029(3)	0.2030(3)	0.2026(4)
	<i>y</i>	$\frac{3}{4}$						
	<i>z</i>	0.5151(8)	0.519(1)	0.522(1)	0.5380(16)	0.5332(11)	0.5366(12)	0.5283(12)
	<i>U</i>	151(17)	163(25)	147(26)	163(17)	158(12)	159(13)	158(15)
O7B	<i>x</i>	0.0447(2)	0.0448(3)	0.0451(4)	0.0467(4)	0.0467(3)	0.0467(4)	0.0466(4)
	<i>y</i>	$\frac{3}{4}$						
	<i>z</i>	0.2194(8)	0.217(1)	0.2220(1)	0.2237(14)	0.2215(11)	0.2233(11)	0.2228(11)
	<i>U</i>	141(16)	137(23)	135(25)	137(16)	146(11)	152(13)	133(14)
T1A	<i>x</i>	0.23168(7)	0.2319(1)	0.2316(1)	0.23111(11)	0.23082(8)	0.23100(9)	0.23102(10)
	<i>y</i>	-0.16299(7)	-0.1636(1)	-0.1633(1)	-0.16485(12)	-0.16492(8)	-0.16488(9)	-0.16460(10)
	<i>z</i>	-0.4491(2)	-0.4481(4)	-0.4461(4)	-0.4373(4)	-0.4373(3)	-0.4377(3)	-0.4402(3)
	<i>U</i>	68(4)	85(6)	64(6)	78(4)	89(3)	86(4)	93(4)
T1B	<i>x</i>	0.01974(7)	0.0199(1)	0.0196(1)	0.01931(11)	0.01909(8)	0.01915(9)	0.01932(10)
	<i>y</i>	-0.16446(7)	-0.1649(1)	-0.1648(1)	-0.16578(11)	-0.16592(8)	-0.16592(9)	-0.16553(9)
	<i>z</i>	0.2987(2)	0.2950(4)	0.2946(4)	0.2820(4)	0.2810(3)	0.2804(3)	0.2845(3)
	<i>U</i>	66(4)	89(6)		93(5)	92(4)	91(4)	91(2)

<i>T2A</i>	<i>x</i>	0.22794(7)	0.2283(1)	0.22277(1)	0.22752(11)	0.22754(8)	0.22740(9)	0.22783(10)	0.22803(4)
	<i>y</i>	-0.07602(7)	-0.07671(1)	-0.0766(1)	-0.07872(12)	-0.07887(8)	-0.07894(9)	-0.07798(10)	-0.07593(5)
	<i>z</i>	0.0516(2)	0.0514(4)	0.0536(4)	0.0611(4)	0.0604(3)	0.0603(3)	0.0582(3)	0.05003(17)
<i>U</i>	<i>x</i>	78(4)	87(6)	79(7)	85(4)	95(3)	89(4)	95(4)	72(2)
<i>T2B</i>	<i>x</i>	0.02663(7)	0.0264(1)	0.0264(1)	0.02541(10)	0.02516(7)	0.02510(9)	0.02542(10)	0.02654(4)
	<i>y</i>	-0.07973(7)	-0.0804(1)	-0.0801(1)	-0.08145(12)	-0.08137(8)	-0.08139(9)	-0.08097(9)	-0.07960(5)
	<i>z</i>	-0.1986(3)	-0.2026(4)	-0.2014(4)	-0.2158(4)	-0.2174(3)	-0.2174(3)	-0.2157(3)	-0.19824(17)
<i>U</i>	<i>x</i>	70(4)	93(6)	67(7)	95(5)	98(3)	98(4)	97(4)	86(2)

TABLE 4c (*contd.*)

	A(19)	A(20)	A(21)	A(22)	A(23)	A(24)	A(25)	A(26)	
<i>M1</i>	<i>x</i>	0.12449(6)	0.12441(1)	0.12445(8)	0.12446(11)	0.12477(8)	0.12478(8)	0.12459(12)	0.12420(5)
	<i>y</i>	0.16074(5)	0.1615(1)	0.16088(7)	0.16210(11)	0.16247(7)	0.16237(7)	0.16238(10)	0.16138(5)
	<i>z</i>	0.3727(2)	0.3757(4)	0.3758(3)	0.3851(4)	0.3863(3)	0.3864(3)	0.3830(4)	0.37165(18)
<i>U</i>	<i>x</i>	102(3)	104(6)	106(5)	95(7)	100(5)	95(5)	97(6)	83(3)
<i>M2</i>	<i>x</i>	0.12452(7)	0.1246(1)	0.1247(1)	0.12477(12)	0.12478(8)	0.12474(9)	0.12473(11)	0.12455(5)
	<i>y</i>	0.07221(6)	0.0724(1)	0.0718(1)	0.07247(12)	0.07237(8)	0.07227(9)	0.07255(10)	0.0722(5)
	<i>z</i>	-0.1286(3)	-0.1257(4)	-0.1252(4)	-0.1148(4)	-0.1141(3)	-0.1137(3)	-0.1173(4)	-0.12973(18)
<i>U</i>	<i>x</i>	63(4)	82(6)	61(6)	92(7)	98(5)	92(5)	83(6)	44(3)
<i>M3</i>	<i>x</i>	0.12460(8)	0.1245(2)	0.1247(1)	0.12491(16)	0.12535(11)	0.12520(12)	0.12529(17)	0.12436(7)
	<i>y</i>	$\frac{1}{4}$							
	<i>z</i>	-0.1273(3)	-0.1261(5)	-0.1246(5)	-0.1156(6)	-0.1137(4)	-0.1137(4)	-0.1173(6)	-0.1282(3)
<i>U</i>	<i>x</i>	81(5)	97(9)	85(7)	102(10)	104(7)	97(7)	87(9)	66(4)
<i>M4</i>	<i>x</i>	0.11912(5)	0.12000(7)	0.11898(7)	0.12211(7)	0.12269(6)	0.12257(6)	0.12197(8)	0.11902(4)
	<i>y</i>	-0.01462(4)	-0.01381(8)	-0.01457(6)	-0.01139(7)	-0.01078(6)	-0.01112(6)	-0.01168(7)	-0.01428(4)
	<i>z</i>	0.3657(2)	0.3702(3)	0.3695(3)	0.3839(2)	0.3835(2)	0.38409(20)	0.3797(3)	0.36379(13)
<i>U</i>	<i>x</i>	126(3)	154(4)	121(4)	131(4)	148(4)	147(4)	135(4)	105(2)
<i>A</i>	<i>x</i>	0.1166(4)	0.1166(7)	0.1147(7)	0.1129(16)	0.1139(15)	0.1129(16)	0.1122(16)	0.1162(3)
	<i>y</i>	$\frac{3}{4}$							
	<i>z</i>	0.847(1)	0.839(2)	0.840(2)	0.842(5)	0.839(5)	0.840(5)	0.838(5)	0.8441(10)
<i>U</i>	<i>x</i>	300	300	300	337(110)	499(100)	518(105)	229(93)	282(19)

Fe^{2+} (A) and Fe^{2+} (B) are well resolved, the average QS of Fe^{2+} (B) ranges from 1.80 to 1.85 mm/s). These values are very close to the QS of Fe^{2+} at the M4 site in anthophyllite–gedrite amphiboles (Hawthorne, 1983), and therefore we assign Fe^{2+} (B) to Fe^{2+} at the M4 site. Fe^{3+} ranges from 3 to 8% of the total Fe in 16 samples of the 25 amphiboles. The observed CS of ~ 0.40 mm/s is characteristic of Fe^{3+} in octahedral coordination. According to Hawthorne (1983), Fe^{3+} preferentially occupies the M2 site in amphiboles, and is so assigned here.

Site populations: general approach

General site-group contents (*A*, *B*, *C* and *T*) are derived from the chemical compositions through the formula-recalculation process, and the electron contents at the various individual sites are derived through site-scattering refinement during crystal-structure refinement. Although these two sets of data are distinct, some of the same information is common to both, and we need to accommodate both sets of data in assigning the site populations while recognizing that both contain systematic errors. With regard to the formulae, the sum of the *B*, *C* and *T* cations is ~ 15.0 a.p.f.u. There is no structural evidence for significant vacancies at the *B*-, *C*- and *T*-sites; hence we normalized the *B*, *C* and *T* cations such that they summed to 15.00 a.p.f.u. (i.e. Na is an *A* cation and is hence excluded) (note that we have not (yet) done this in Table 3) when assigning site populations.

Next, let us consider the refined site-scattering values (Table 6). These are very precise, but their accuracy depends on scaling the cation-scattering to the rest of the scattering of the structure, i.e. the scattering from the anions. This process is dependent on the specific scattering factor used for oxygen: (1) neutral; (2) ionized; or (3) partly ionized (a mixture of (1) and (2)). Here, we used an ionized scattering-factor for oxygen. Recognizing that the relative accuracy of the refined site-scattering values is greater than their absolute accuracy, we have overcome this difficulty by normalizing the site-scattering values to the electron sum of the cations in the normalized unit formula. The relative values of (1) the cation contents of the unit formulae; and (2) the site-scattering values, are more accurate than their absolute values. Here, we take advantage of this greater relative accuracy by scaling the absolute values of the cation content

and the sum of the site-scattering values to the structural constraint that vacancies do not occur at the sites occupied by the *B*, *C* and *T* cations. The resultant site-populations for all sites in the anthophyllite–gedrite crystals of this work, derived from the arguments given below, are given in Tables 8 and 9.

Site populations: the *T*sites

Substitution of Al for Si in the tetrahedral double-chain is a major compositional feature of the orthorhombic amphiboles. The Al content of the *T* sites in orthorhombic amphiboles varies in the range 0.0–2.5 a.p.f.u., although compositions extremely rich in $[{}^4\text{Al}]$ are uncommon. The X-ray scattering factors of Al and Si are very similar, and direct determination of Al-Si site-populations by least-squares refinement of X-ray data is accompanied by high parameter correlation and concomitantly large standard deviations; in addition, the final refined values will be extremely sensitive to any systematic error in the data. In principle, this problem may be reduced by using high-angle X-ray data, but this has not been an effective method for Al-Si site-population determination, and we must rely on crystal-chemical analysis.

Total $[{}^4\text{Al}]$

The amount of $[{}^4\text{Al}$ (tetrahedrally coordinated Al) is determined directly from the calculation of the unit formula from the chemical composition. As Si and Al have different empirical radii (0.26 and 0.39 Å, respectively; Shannon, 1976), the $\langle\langle \text{T}-\text{O} \rangle\rangle$ distance (grand-mean bond-length) should be linearly related to the amount of $[{}^4\text{Al}]$. This point is examined in Fig. 4; the results of regression analysis are as follows: $\langle\langle \text{T}-\text{O} \rangle\rangle = 1.6214(8) + 0.0171(6) [{}^4\text{Al}]$; $R = 0.985$. The data form a linear trend with a slope that is not significantly different from that characteristic of a hard-sphere model.

Assignment to individual *T* sites

There are four symmetrically distinct cation sites with tetrahedral coordination in the orthorhombic (*Pnma*) amphibole structure: T1*A*, T2*A*, T1*B* and T2*B* (Fig. 1). The variation in individual $\langle\langle \text{T}-\text{O} \rangle\rangle$ distances is not linear as a function of total $[{}^4\text{Al}]$, and we need to develop relations to assign Al contents to the individual *T* sites.

TABLE 5a. Selected interatomic distances (\AA) for anthophyllites and gedrites of this work [samples A(1)–A(13)].

	A(1)	A(2)	A(3)	A(5)	A(6)	A(7)	A(8)	A(9)	A(10)	A(11)	A(12)	A(13)
T1A–O1A	1.652(2)	1.658(2)	1.640(7)	1.607(2)	1.643(6)	1.658(3)	1.657(6)	1.660(5)	1.660(3)	1.627(15)	1.654(6)	1.644(6)
T1A–O5A	1.659(2)	1.664(2)	1.660(7)	1.638(2)	1.658(6)	1.666(3)	1.662(6)	1.670(5)	1.661(3)	1.707(13)	1.661(5)	1.663(6)
T1A–O6A	1.641(2)	1.643(2)	1.626(7)	1.618(2)	1.620(6)	1.645(3)	1.614(5)	1.650(5)	1.648(3)	1.629(13)	1.635(5)	1.645(6)
T1A–O7A	1.641(1)	1.645(1)	1.641(4)	1.616(1)	1.642(4)	1.645(2)	1.642(4)	1.641(3)	1.647(2)	1.632(9)	1.640(3)	1.640(4)
<T1A–O>	1.648(2)	1.653(2)	1.642(6)	1.620(2)	1.641(6)	1.654(3)	1.644(5)	1.655(5)	1.654(3)	1.649(13)	1.648(5)	1.648(6)
T1B–O1B	1.667(2)	1.675(2)	1.678(7)	1.611(2)	1.639(6)	1.674(3)	1.643(6)	1.674(5)	1.672(3)	1.688(16)	1.644(6)	1.653(7)
T1B–O5B	1.672(2)	1.681(2)	1.678(7)	1.638(2)	1.662(7)	1.683(3)	1.662(6)	1.688(5)	1.686(3)	1.663(15)	1.664(6)	1.671(6)
T1B–O6B	1.659(2)	1.665(2)	1.658(5)	1.624(2)	1.644(6)	1.668(3)	1.654(6)	1.667(5)	1.663(3)	1.654(12)	1.643(5)	1.653(7)
T1B–O7B	1.650(1)	1.652(1)	1.657(5)	1.621(2)	1.626(4)	1.656(2)	1.625(3)	1.651(3)	1.652(2)	1.658(11)	1.632(3)	1.636(4)
<T1B–O>	1.662(2)	1.668(2)	1.624(2)	1.668(6)	1.643(6)	1.670(3)	1.646(5)	1.670(5)	1.668(3)	1.666(14)	1.646(5)	1.653(6)
T2A–O2A	1.627(2)	1.629(2)	1.616(7)	1.626(6)	1.629(2)	1.632(6)	1.629(4)	1.629(3)	1.614(14)	1.630(5)	1.635(6)	
T2A–O4A	1.599(2)	1.600(2)	1.593(7)	1.597(2)	1.610(6)	1.607(3)	1.610(6)	1.603(5)	1.601(3)	1.592(15)	1.611(5)	1.599(6)
T2A–O5A	1.657(2)	1.656(2)	1.660(7)	1.661(2)	1.654(6)	1.650(3)	1.651(5)	1.653(5)	1.657(3)	1.628(13)	1.661(5)	1.667(6)
T2A–O6A	1.621(2)	1.620(2)	1.639(7)	1.624(2)	1.634(6)	1.626(3)	1.637(6)	1.618(5)	1.618(3)	1.658(13)	1.627(5)	1.627(6)
<T2A–O>	1.626(2)	1.626(2)	1.627(7)	1.623(2)	1.631(6)	1.628(3)	1.633(6)	1.627(5)	1.626(3)	1.623(14)	1.632(5)	1.632(6)
T2B–O2B	1.666(2)	1.668(2)	1.670(7)	1.625(2)	1.658(6)	1.670(2)	1.650(6)	1.668(4)	1.664(3)	1.676(14)	1.650(5)	1.658(6)
T2B–O4B	1.634(2)	1.637(2)	1.644(7)	1.607(2)	1.618(6)	1.637(3)	1.614(6)	1.632(5)	1.637(3)	1.646(16)	1.619(5)	1.604(6)
T2B–O5B	1.672(2)	1.676(2)	1.664(7)	1.646(2)	1.664(7)	1.676(3)	1.663(6)	1.669(5)	1.670(3)	1.678(14)	1.658(5)	1.668(6)
T2B–O6B	1.658(2)	1.661(2)	1.649(7)	1.653(2)	1.662(6)	1.657(3)	1.651(6)	1.659(5)	1.658(3)	1.635(13)	1.662(5)	1.655(6)
<T2B–O>	1.658(2)	1.661(2)	1.657(7)	1.633(2)	1.651(6)	1.660(3)	1.644(6)	1.657(5)	1.657(3)	1.659(14)	1.647(5)	1.646(6)
<<T–O>>	1.649(2)	1.652(2)	1.649(7)	1.625(2)	1.641(6)	1.653(3)	1.642(6)	1.652(5)	1.651(3)	1.649(14)	1.643(5)	1.645(6)
M1–O1A	2.063(2)	2.062(2)	2.071(6)	2.063(2)	2.052(6)	2.068(2)	2.052(5)	2.064(4)	2.060(3)	2.101(12)	2.048(5)	2.057(6)
M1–O1B	2.057(2)	2.058(2)	2.052(7)	2.060(2)	2.081(6)	2.059(2)	2.078(5)	2.061(4)	2.056(3)	2.065(12)	2.084(5)	2.072(6)
M1–O2A	2.138(2)	2.154(2)	2.160(7)	2.110(2)	2.139(6)	2.156(5)	2.136(5)	2.151(4)	2.151(3)	2.166(13)	2.140(5)	2.123(6)
M1–O2B	2.149(2)	2.164(2)	2.169(7)	2.130(2)	2.141(6)	2.170(3)	2.152(6)	2.167(4)	2.166(3)	2.185(14)	2.156(5)	2.151(6)
M1–O3A	2.093(2)	2.100(2)	2.111(6)	2.084(2)	2.091(6)	2.098(2)	2.092(5)	2.096(4)	2.098(3)	2.112(13)	2.095(5)	2.084(6)
M1–O3B	2.063(2)	2.066(2)	2.070(6)	2.067(6)	2.069(2)	2.068(5)	2.068(5)	2.071(4)	2.069(2)	2.070(12)	2.073(5)	2.059(6)
<M1–O>	2.094(2)	2.101(2)	2.106(7)	2.086(2)	2.095(6)	2.103(2)	2.096(5)	2.102(4)	2.100(3)	2.117(13)	2.099(5)	2.091(5)

TABLE 5a (contd.)

	A(1)	A(2)	A(3)	A(5)	A(6)	A(7)	A(8)	A(9)	A(10)	A(11)	A(12)	A(13)
<i>M</i> 2-01A	2.040(2)	2.025(2)	2.058(7)	2.132(2)	2.071(6)	2.024(3)	2.071(6)	2.027(5)	2.033(3)	2.058(16)	2.078(5)	2.089(6)
<i>M</i> 2-01B	2.028(2)	2.012(2)	2.028(7)	2.120(2)	2.061(6)	2.017(3)	2.065(6)	2.022(5)	2.026(3)	2.022(17)	2.060(5)	2.051(6)
<i>M</i> 2-02A	1.999(2)	1.993(2)	2.003(7)	2.063(2)	2.002(6)	1.992(3)	2.010(5)	1.996(4)	2.001(3)	2.009(12)	2.006(5)	2.015(6)
<i>M</i> 2-02B	2.013(2)	2.011(2)	2.023(7)	2.075(2)	2.046(6)	2.012(3)	2.053(5)	2.017(5)	2.021(3)	2.029(14)	2.057(5)	2.066(6)
<i>M</i> 2-04A	1.933(2)	1.928(2)	1.947(7)	2.008(2)	1.942(6)	1.924(3)	1.945(6)	1.924(5)	1.935(3)	1.952(14)	1.943(5)	1.955(6)
<i>M</i> 2-04B	1.948(2)	1.943(2)	1.950(7)	2.033(2)	1.961(6)	1.939(3)	1.975(6)	1.943(5)	1.947(3)	1.951(15)	1.964(5)	1.982(6)
$\langle M2-O \rangle$	1.994(2)	1.985(2)	2.002(7)	2.072(2)	2.014(6)	1.985(3)	2.020(6)	1.988(5)	1.994(3)	2.004(15)	2.018(5)	2.026(6)
<i>M</i> 3-01A $\times 2$	2.091(2)	2.104(2)	2.110(7)	2.085(2)	2.103(6)	2.105(3)	2.084(6)	2.104(5)	2.103(3)	2.106(15)	2.086(5)	2.075(6)
<i>M</i> 3-01B $\times 2$	2.097(2)	2.110(2)	2.118(7)	2.085(2)	2.102(6)	2.112(3)	2.096(6)	2.106(5)	2.110(3)	2.118(16)	2.098(5)	2.075(6)
<i>M</i> 3-03A	2.049(2)	2.053(3)	2.057(9)	2.053(3)	2.049(8)	2.053(4)	2.049(8)	2.053(6)	2.054(4)	2.040(19)	2.040(7)	2.032(9)
<i>M</i> 3-03B	2.044(2)	2.046(3)	2.063(9)	2.049(3)	2.075(8)	2.051(4)	2.061(8)	2.050(6)	2.046(4)	2.073(18)	2.068(7)	2.040(9)
$\langle M3-O \rangle$	2.078(2)	2.088(2)	2.096(8)	2.074(3)	2.089(7)	2.091(3)	2.078(7)	2.087(5)	2.087(3)	2.094(17)	2.079(6)	2.062(7)
<i>M</i> 4-02A	2.237(2)	2.243(2)	2.239(6)	2.175(2)	2.221(6)	2.247(3)	2.197(5)	2.242(4)	2.245(3)	2.239(13)	2.204(5)	2.163(6)
<i>M</i> 4-02B	2.122(2)	2.120(2)	2.124(6)	2.139(2)	2.131(6)	2.120(3)	2.119(5)	2.123(4)	2.126(3)	2.127(14)	2.118(5)	2.078(6)
<i>M</i> 4-04A	2.124(2)	2.130(2)	2.120(6)	2.048(2)	2.099(6)	2.133(2)	2.093(5)	2.135(4)	2.131(3)	2.134(13)	2.092(5)	2.084(7)
<i>M</i> 4-04B	2.019(2)	2.018(2)	1.998(6)	1.998(2)	2.012(6)	2.025(2)	2.014(5)	2.023(4)	2.024(3)	2.005(13)	2.016(5)	2.021(7)
<i>M</i> 4-05A	2.259(2)	2.251(2)	2.294(6)	2.391(2)	2.297(6)	2.255(3)	2.293(6)	2.253(4)	2.262(3)	2.280(13)	2.278(5)	2.239(6)
<i>M</i> 4-05B	2.454(2)	2.416(2)	2.489(7)	2.842(3)	2.581(7)	2.417(3)	2.601(6)	2.422(4)	2.436(3)	2.528(14)	2.604(5)	2.565(6)
<i>M</i> 4-06B	2.915(2)	2.938(2)	2.939(7)	2.858(3)	2.899(7)	2.938(3)	2.897(6)	2.936(4)	2.933(3)	2.896(5)	2.969(6)	
$\langle [7]M4-O \rangle$	2.304(2)	2.302(2)	2.315(6)	2.349(2)	2.320(6)	2.305(3)	2.316(6)	2.305(4)	2.308(3)	2.323(13)	2.315(5)	2.303(6)
<i>A</i> -06A $\times 2$	2.665(3)	2.656(3)	2.662(11)	—	2.678(14)	2.654(4)	2.676(15)	2.646(7)	2.661(4)	2.654(22)	2.666(12)	2.609(11)
<i>A</i> -06B $\times 2$	2.614(3)	2.621(3)	2.651(13)	—	2.676(16)	2.624(4)	2.701(16)	2.628(7)	2.630(4)	2.674(23)	2.686(14)	2.642(12)
<i>A</i> -07A	2.366(5)	2.392(5)	2.348(18)	—	2.319(22)	2.387(6)	2.358(23)	2.361(1)	2.383(6)	2.348(33)	2.337(19)	2.340(17)
<i>A</i> -07B	2.377(5)	2.378(5)	2.368(18)	—	2.411(22)	2.378(6)	2.364(22)	2.40(1)	2.379(6)	2.413(33)	2.398(19)	2.385(17)
$\langle A-O \rangle$	2.550(4)	2.554(4)	2.557(14)	—	2.573(17)	2.554(5)	2.579(18)	2.552(8)	2.557(5)	2.570(26)	2.573(15)	2.538(13)

Table 5 continues on next page

TABLE 5b. Selected interatomic distances (\AA) for anthophyllites and gedrites of this work [samples A(14)–A(26)].

	A(14)	A(15)	A(16)	A(17)	A(18)	A(19)	A(20)	A(21)	A(22)	A(23)	A(24)	A(25)	A(26)
T1A–O1A	1.648(4)	1.638(6)	1.660(3)	1.656(8)	1.615(3)	1.662(3)	1.634(5)	1.651(5)	1.626(6)	1.628(4)	1.627(5)	1.628(5)	1.659(2)
T1A–O5A	1.664(3)	1.648(7)	1.667(3)	1.660(7)	1.636(3)	1.672(3)	1.655(5)	1.667(5)	1.646(6)	1.646(4)	1.648(4)	1.648(4)	1.666(2)
T1A–O6A	1.635(3)	1.631(7)	1.650(3)	1.616(7)	1.612(3)	1.645(3)	1.629(5)	1.633(5)	1.630(6)	1.626(4)	1.632(4)	1.625(6)	1.649(2)
T1A–O7A	1.644(2)	1.637(4)	1.651(2)	1.646(5)	1.621(2)	1.648(2)	1.644(3)	1.643(3)	1.620(3)	1.626(2)	1.627(3)	1.629(3)	1.645(1)
<T1A–O>	1.648(3)	1.639(6)	1.657(3)	1.645(7)	1.621(3)	1.657(3)	1.641(5)	1.649(5)	1.631(6)	1.632(4)	1.634(4)	1.633(5)	1.655(2)
T1B–O1B	1.664(4)	1.659(6)	1.677(4)	1.616(8)	1.610(4)	1.672(3)	1.666(5)	1.665(5)	1.637(5)	1.636(4)	1.635(5)	1.635(5)	1.677(2)
T1B–O5B	1.674(4)	1.655(7)	1.688(3)	1.654(8)	1.638(3)	1.686(3)	1.659(5)	1.683(5)	1.634(6)	1.644(4)	1.640(4)	1.642(5)	1.686(2)
T1B–O6B	1.652(4)	1.638(7)	1.665(3)	1.658(7)	1.627(3)	1.663(4)	1.658(5)	1.653(5)	1.624(6)	1.626(4)	1.631(5)	1.628(5)	1.668(2)
T1B–O7B	1.648(2)	1.625(4)	1.657(2)	1.625(4)	1.621(2)	1.650(2)	1.639(3)	1.645(3)	1.628(4)	1.630(2)	1.629(3)	1.631(3)	1.655(1)
<T1B–O>	1.660(4)	1.644(6)	1.672(3)	1.638(7)	1.624(3)	1.668(3)	1.656(5)	1.662(5)	1.631(5)	1.634(4)	1.634(4)	1.635(5)	1.672(2)
T2A–O2A	1.628(4)	1.611(6)	1.635(3)	1.641(7)	1.618(3)	1.629(3)	1.618(5)	1.631(5)	1.614(5)	1.618(4)	1.620(5)	1.622(5)	1.627(2)
T2A–O4A	1.602(4)	1.608(6)	1.605(3)	1.614(7)	1.597(3)	1.604(3)	1.603(5)	1.609(5)	1.594(6)	1.594(6)	1.597(5)	1.600(5)	1.603(2)
T2A–O5A	1.658(3)	1.678(7)	1.658(3)	1.649(7)	1.665(3)	1.657(3)	1.664(5)	1.653(5)	1.658(6)	1.667(4)	1.661(4)	1.668(5)	1.655(2)
T2A–O6A	1.630(3)	1.627(7)	1.622(3)	1.642(7)	1.628(3)	1.625(3)	1.631(5)	1.625(5)	1.617(6)	1.620(4)	1.618(4)	1.629(5)	1.618(2)
<T2A–O>	1.630(4)	1.631(7)	1.630(3)	1.637(7)	1.627(3)	1.629(3)	1.629(5)	1.630(5)	1.621(6)	1.626(4)	1.624(4)	1.630(5)	1.626(2)
T2B–O2B	1.664(4)	1.660(6)	1.665(3)	1.632(7)	1.629(3)	1.662(3)	1.668(5)	1.663(5)	1.641(5)	1.641(4)	1.638(4)	1.647(5)	1.666(2)
T2B–O4B	1.622(4)	1.610(7)	1.630(4)	1.614(7)	1.597(3)	1.629(3)	1.630(5)	1.633(5)	1.614(6)	1.613(4)	1.611(4)	1.613(4)	1.629(2)
T2B–O5B	1.665(4)	1.653(7)	1.664(3)	1.660(7)	1.645(3)	1.666(3)	1.672(5)	1.657(5)	1.651(6)	1.644(4)	1.649(4)	1.656(5)	1.669(2)
T2B–O6B	1.655(4)	1.661(7)	1.655(4)	1.650(8)	1.651(3)	1.654(3)	1.650(6)	1.657(5)	1.661(6)	1.656(4)	1.659(5)	1.665(5)	1.654(2)
<T2B–O>	1.652(4)	1.646(7)	1.653(4)	1.639(7)	1.631(3)	1.653(3)	1.655(5)	1.653(5)	1.642(6)	1.639(4)	1.639(4)	1.645(5)	1.655(2)
<<T–O>>	1.647(4)	1.653(3)	1.640(7)	1.640(7)	1.626(3)	1.652(3)	1.645(5)	1.648(5)	1.631(6)	1.633(4)	1.633(4)	1.636(5)	1.652(2)
M1–O1A	2.067(3)	2.053(6)	2.066(3)	2.050(7)	2.069(3)	2.064(3)	2.065(5)	2.072(5)	2.051(6)	2.059(6)	2.061(4)	2.054(5)	2.060(2)
M1–O1B	2.056(3)	2.080(6)	2.060(3)	2.092(7)	2.067(3)	2.062(3)	2.051(5)	2.073(5)	2.062(5)	2.059(4)	2.067(4)	2.061(5)	2.058(2)
M1–O2A	2.137(3)	2.142(6)	2.146(3)	2.128(7)	2.116(3)	2.154(3)	2.130(5)	2.156(5)	2.137(5)	2.130(4)	2.139(4)	2.126(5)	2.143(2)
M1–O2B	2.154(3)	2.145(7)	2.170(3)	2.158(7)	2.142(3)	2.176(3)	2.143(5)	2.172(5)	2.134(6)	2.146(4)	2.148(4)	2.137(5)	2.157(2)
M1–O3A	2.09(3)	2.104(6)	2.105(3)	2.087(7)	2.084(3)	2.100(3)	2.091(5)	2.109(5)	2.103(5)	2.098(4)	2.101(4)	2.100(5)	2.091(2)
M1–O3B	2.061(3)	2.058(6)	2.077(3)	2.092(7)	2.073(3)	2.069(3)	2.056(5)	2.074(4)	2.073(5)	2.077(4)	2.079(4)	2.074(4)	2.061(2)
<M1–O>	2.094(3)	2.097(6)	2.104(3)	2.101(7)	2.092(3)	2.104(3)	2.089(5)	2.109(5)	2.093(5)	2.095(4)	2.099(4)	2.092(5)	2.095(2)

GEDRITE CRYSTAL CHEMISTRY. 1. CRYSTAL STRUCTURE

TABLE 5b (contd.)

	A(14)	A(15)	A(16)	A(17)	A(18)	A(19)	A(20)	A(21)	A(22)	A(23)	A(24)	A(25)	A(26)
<i>M</i> 2-O1A	2.054(4)	2.094(7)	2.046(4)	2.097(7)	2.137(3)	2.040(3)	2.066(5)	2.050(5)	2.120(6)	2.126(4)	2.126(5)	2.115(5)	2.038(2)
<i>M</i> 2-O1B	2.034(4)	2.050(7)	2.031(3)	2.097(7)	2.120(3)	2.019(3)	2.050(5)	2.031(5)	2.100(5)	2.110(4)	2.110(4)	2.091(5)	2.019(2)
<i>M</i> 2-O2A	2.001(3)	2.012(6)	2.004(3)	2.018(7)	2.071(3)	1.994(3)	2.017(5)	1.993(5)	2.041(5)	2.053(4)	2.059(4)	2.033(5)	2.002(2)
<i>M</i> 2-O2B	2.031(3)	2.058(7)	2.034(3)	2.077(7)	2.082(3)	2.024(3)	2.034(5)	2.029(5)	2.063(6)	2.072(4)	2.073(4)	2.064(5)	2.020(2)
<i>M</i> 2-O4A	1.935(4)	1.954(6)	1.931(3)	1.959(7)	2.006(3)	1.928(3)	1.936(5)	1.930(5)	2.002(6)	1.994(4)	2.000(5)	1.974(5)	1.923(2)
<i>M</i> 2-O4B	1.958(4)	1.971(7)	1.956(3)	1.996(7)	2.042(3)	1.946(3)	1.964(5)	1.943(5)	2.007(6)	2.013(4)	2.014(4)	1.995(5)	1.947(2)
< <i>M</i> 2-O>	2.002(4)	2.023(7)	2.000(3)	2.041(7)	2.076(3)	1.992(3)	2.011(5)	1.996(5)	2.056(6)	2.061(4)	2.064(4)	2.045(5)	1.992(2)
<i>M</i> 3-O1A × 2	2.088(4)	2.079(7)	2.091(3)	2.073(7)	2.082(3)	2.090(3)	2.091(5)	2.101(5)	2.095(6)	2.087(4)	2.094(4)	2.084(5)	2.082(2)
<i>M</i> 3-O1B × 2	2.096(4)	2.084(7)	2.099(3)	2.111(7)	2.095(3)	2.108(3)	2.083(5)	2.105(5)	2.084(5)	2.086(4)	2.090(4)	2.084(5)	2.088(2)
<i>M</i> 3-O3A	2.037(5)	2.029(9)	2.040(5)	2.04(1)	2.052(4)	2.047(5)	2.050(7)	2.039(7)	2.039(8)	2.051(6)	2.051(6)	2.048(7)	2.049(3)
<i>M</i> 3-O3B	2.052(5)	2.060(9)	2.041(5)	2.08(1)	2.062(4)	2.051(5)	2.051(7)	2.053(7)	2.063(8)	2.053(5)	2.061(6)	2.068(6)	2.037(3)
< <i>M</i> 3-O>	2.076(4)	2.069(8)	2.077(4)	2.081(8)	2.078(3)	2.078(3)	2.082(4)	2.075(6)	2.084(5)	2.077(6)	2.075(5)	2.075(6)	2.071(2)
<i>M</i> 4-O2A	2.218(3)	2.205(6)	2.230(3)	2.185(7)	2.157(3)	2.229(3)	2.215(5)	2.238(4)	2.189(5)	2.172(4)	2.172(4)	2.186(4)	2.223(2)
<i>M</i> 4-O2B	2.108(3)	2.108(6)	2.116(3)	2.139(7)	2.126(3)	2.113(3)	2.119(5)	2.111(5)	2.139(5)	2.121(4)	2.131(4)	2.120(4)	2.106(2)
<i>M</i> 4-O4A	2.115(3)	2.105(6)	2.126(3)	2.075(7)	2.045(3)	2.123(3)	2.123(5)	2.108(5)	2.053(6)	2.062(4)	2.065(4)	2.084(5)	2.126(2)
<i>M</i> 4-O4B	2.019(3)	2.021(6)	2.027(3)	2.011(7)	1.998(3)	2.022(3)	1.999(5)	2.017(5)	1.993(5)	1.994(4)	2.004(4)	2.004(4)	2.021(2)
<i>M</i> 4-O5A	2.247(3)	2.276(6)	2.245(3)	2.329(7)	2.386(3)	2.235(3)	2.276(5)	2.276(4)	2.362(6)	2.353(4)	2.368(4)	2.322(5)	2.238(2)
<i>M</i> 4-O5B	2.505(4)	2.602(7)	2.462(4)	2.668(8)	2.870(3)	2.448(3)	2.512(5)	2.498(5)	2.773(6)	2.795(4)	2.802(5)	2.771(5)	2.420(2)
<i>M</i> 4-O6B	2.928(4)	2.922(6)	2.944(4)	2.928(8)	2.872(3)	2.942(3)	2.930(5)	2.898(5)	2.885(5)	2.868(5)	2.890(5)	2.890(5)	2.939(3)
<[7] <i>M</i> 4-O>	2.306(3)	2.320(6)	2.307(3)	2.334(7)	2.351(3)	2.302(3)	2.311(5)	2.307(5)	2.339(6)	2.340(4)	2.344(4)	2.340(4)	2.296(2)
<i>A</i> -O6A × 2	2.655(6)	2.637(12)	2.652(5)	2.672(14)	2.677(38)	2.643(5)	2.646(9)	2.682(9)	2.710(19)	2.693(17)	2.711(18)	2.701(19)	2.640(4)
<i>A</i> -O6B × 2	2.637(7)	2.661(14)	2.644(5)	2.695(15)	2.808(39)	2.647(6)	2.663(10)	2.654(10)	2.736(23)	2.747(21)	2.748(21)	2.684(20)	2.617(5)
<i>A</i> -O7A	2.361(9)	2.305(21)	2.376(7)	2.303(22)	2.28(58)	2.389(8)	2.323(14)	2.363(15)	2.328(28)	2.313(26)	2.322(24)	2.344(27)	2.377(6)
<i>A</i> -O7B	2.368(9)	2.459(20)	2.364(7)	2.409(21)	2.370(55)	2.378(8)	2.403(13)	2.391(15)	2.365(28)	2.378(26)	2.374(23)	2.371(26)	2.352(6)
< <i>A</i> -O>	2.552(7)	2.560(16)	2.555(6)	2.574(17)	2.592(44)	2.558(6)	2.547(11)	2.571(11)	2.598(24)	2.595(22)	2.602(21)	2.581(22)	2.541(5)

TABLE 6. Refined site-scattering values* (e.p.f.u.) for cation sites in orthorhombic amphiboles.

	A(1)	A(2)	A(3)	A(5)	A(6)	A(7)	A(8)	A(9)	A(10)	A(11)	A(12)	A(13)	A(14)
M1	29.4(1)	32.5(1)	35.1(2)	26.5(1)	29.1(2)	32.7(1)	32.3(2)	32.5(2)	32.5(1)	38.8(4)	32.5(2)	25.3(2)	31.6(1)
M2	25.8(1)	25.2(1)	27.0(2)	24.9(1)	26.8(2)	26.1(1)	28.1(2)	26.3(2)	27.2(1)	29.6(4)	27.9(2)	25.1(2)	27.0(1)
M3	15.1(1)	16.9(1)	18.4(2)	12.8(1)	15.4(2)	17.4(1)	15.6(1)	16.7(1)	17.0(1)	18.4(3)	15.8(1)	12.2(1)	15.3(1)
M4	40.9(1)	42.8(1)	47.8(2)	45.0(1)	45.0(2)	42.4(1)	40.6(2)	42.5(2)	43.9(1)	46.4(4)	40.6(2)	26.1(2)	38.8(1)
ΣM	111.2	117.4	128.3	109.2	116.3	118.6	116.6	118.0	120.6	133.2	116.8	88.7	112.7
EMPA	111.8	117.5	127.8	108.2	115.9	119.2	117.0	118.7	120.7	132.3	116.4	89.2	112.1
ΣA	4.9(1)	5.8(1)	4.5(1)	0.0	2.7(2)	5.9(1)	3.4(1)	5.8(1)	6.0(1)	5.0(2)	3.5(1)	3.9(1)	5.2(1)
EMPA	4.8	5.9	4.2	0.4	3.0	5.4	3.0	5.3	5.7	4.2	3.0	4.0	5.2
	A(15)	A(16)	A(17)	A(18)	A(19)	A(20)	A(21)	A(22)	A(23)	A(24)	A(25)	A(26)	
M1	29.3(2)	34.8(1)	33.1(3)	28.3(1)	34.3(1)	27.5(2)	36.9(1)	28.4(2)	29.9(2)	31.7(2)	25.1(2)	26.6(1)	
M2	25.8(2)	28.1(1)	28.8(2)	26.5(1)	27.0(1)	25.9(2)	28.4(1)	25.9(2)	27.4(2)	28.6(2)	24.3(2)	24.3(1)	
M3	13.9(2)	16.9(1)	16.0(2)	13.8(1)	16.9(1)	13.6(1)	18.0(1)	14.2(2)	14.6(1)	15.5(1)	12.3(2)	13.4(1)	
M4	36.4(2)	41.4(1)	42.4(3)	39.4(1)	40.4(1)	38.7(2)	44.1(2)	47.2(2)	40.1(2)	42.8(2)	37.5(2)	35.5(1)	
ΣM	105.4	121.2	120.3	108.0	118.6	105.7	127.4	115.7	112.0	118.6	99.2	99.8	
EMPA	105.6	120.5	118.8	107.4	118.0	105.5	126.6	115.8	112.0	117.6	101.2	101.9	
ΣA	4.0(1)	6.4(1)	4.3(2)	0.5(1)	5.9(1)	4.0(1)	4.5(1)	2.0(2)	1.8(1)	2.3(1)	1.6(2)	4.6(1)	
EMPA	3.7	6.2	4.4	0.5	5.6	4.0	3.6	2.4	2.0	2.5	2.3	5.5	

TABLE 7. Selected hyperfine parameters at RT for the anthophyllite–gedrite amphiboles.

Sample	Fe ²⁺ (A)			Fe ²⁺ (B)			Fe ³⁺		
	CS (mm/s)	QS (mm/s)	A (%)	CS (mm/s)	QS (mm/s)	A (%)	CS (mm/s)	QS (mm/s)	A (%)
A2	1.18	2.39	59	1.14	1.94	37	0.40*	0.76	4
A5	1.18	2.70	18	1.14	1.85	82	—	—	—
A6	1.17	2.47	49	1.13	1.86	45	0.40	0.55	6
A7	1.16	2.41	60	1.14	1.91	32	0.40	0.62	8
A8	1.16	2.53	54	1.14	1.86	41	0.40*	0.59	5
A10	1.16	2.47	59	1.14	1.88	33	0.40	0.57	8
A11	1.14	2.66	53	1.12	1.90	41	0.36	0.94	6
A13	1.16	2.50	40	1.15	1.96	52	0.42	0.82	8
A15	1.16	2.51	56	1.14	1.88	41	0.40*	0.61	3
A16	1.16	2.49	55	1.14	1.99	39	0.40	0.64	6
A18	1.16	2.76	38	1.13	1.83	62	—	—	—
A20	1.18	2.37	54	1.13	1.87	46	—	—	—
A22	1.16	2.60	34	1.13	1.85	62	0.40*	0.59	4
A23	1.17	2.54	36	1.14	1.84	61	0.36*	0.70*	3
A24	1.16	2.64	39	1.13	1.83	58	0.36*	0.70*	3
A25	1.17	2.54	26	1.14	1.88	68	0.36*	0.70*	6
A26	1.17	2.31	43	1.14	1.89	57	—	—	—
138342	1.16	2.53	52	1.13	1.90	45	0.40*	0.61*	3
UBC89	1.16	2.50	49	1.14	2.04	48	0.40*	0.61*	3
UBC92	1.15	2.54	59	1.12	1.80	35	0.40*	0.61*	6

* Fixed parameter

There is crystal-structure information available for the following $^{[4]}Al$ -poor amphiboles: A(5) and A(18) of this study; anthophyllite[23] of Finger (1970), see Hawthorne (1983); and the anthophyllite of Walitzi *et al.* (1989). Inspection of the $\langle T-O \rangle$ distances in these amphiboles shows that $\langle T2B-O \rangle$ at $\sim 1.633 \text{ \AA}$ is significantly larger than $\langle T1A-O \rangle$ at 1.621 , $\langle T2A-O \rangle$ at 1.623 , and $\langle T1B-O \rangle$ at 1.625 \AA . There are two possibilities here: (1) all $^{[4]}Al$ is ordered at the $T2B$ site in the anthophyllite; (2) $\langle T2B-O \rangle$ is intrinsically longer than the other T polyhedra in orthorhombic amphiboles. Possibility (2) is quite reasonable as $\langle T(2)-O \rangle$ is significantly longer than $\langle T(2)-O \rangle$ in $^{[4]}Al$ -free monoclinic amphiboles (Oberti *et al.*, 1995). We will assign $^{[4]}Al$ to the T sites in the anthophyllite structures according to the differences in $\langle T-O \rangle$ distances between these and the most $^{[4]}Al$ -rich amphibole [A(9), Table 3], and then extrapolate the $\langle T-O \rangle$ distances to zero occupancy of Al. The resulting distances are as follows: $\langle T1A-O \rangle = 1.616$, $\langle T2A-O \rangle = 1.624$, $\langle T1B-O \rangle = 1.617$, and $\langle T2B-O \rangle = 1.630 \text{ \AA}$. The resulting mean value is 1.622 \AA , which agrees reasonably well with the grand $\langle T-O \rangle$ distance of $1.621(1) \text{ \AA}$ for $^{[4]}Al$ -free $Pnma$ amphiboles derived from Fig. 4. Assuming that the individual T sites behave in a similar way as a function of $^{[4]}Al$, we may assign Al contents to each of the T sites using the mean distances for zero occupancy given above, together with the slope of the regression line given above (multiplied by 4 to account for the difference in the number of sites); the resultant site-populations are given in Table 8.

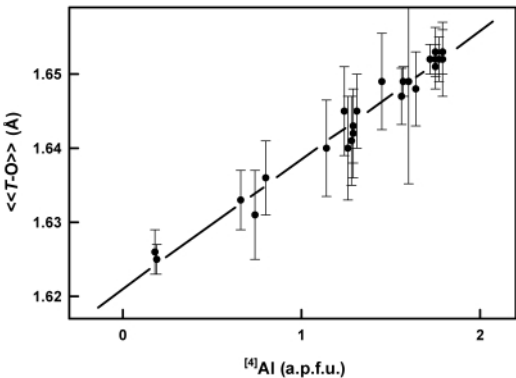


FIG. 4. Variation in grand mean $T-O$ distance, $\langle\langle T-O \rangle\rangle$, as a function of $^{[4]}Al$ content in a.p.f.u.; the regression line (Table 8) is shown.

Site populations: the M sites

There are four M sites that are occupied by the small- to intermediate-sized ($0.535-0.83 \text{ \AA}$) cations (Al, Ti^{4+} , Fe^{3+} , Fe^{2+} , Mn^{2+} , Mg and Ca, Table 3), and site populations may be assigned on the basis of the refined site-scattering values (Table 6) and the observed $\langle M-O \rangle$ distances. First, let us compare the total scattering at the M sites as derived from the site-scattering results with the analogous effective scattering calculated from the aggregate M -site contents as derived from the chemical compositions (Fig. 5). There is a 1:1 relation between these two quantities, with no significant outliers. Hawthorne (1983) has shown that the grand mean bond-length at $M1$, $M2$ and $M3$ sites, $\langle M^{1,2,3}-O \rangle$, correlates strongly with the grand mean radius of the constituent cations at these sites, $\langle r^{M1,2,3} \rangle$. Figure 6 shows that this is the case for the data presented here. Linear regression gives a correlation coefficient, $R = 0.973$, and the resulting equation is shown in

TABLE 8. Assigned Al site-populations at the T sites in orthorhombic amphiboles.

	T1A	T2A	T1B	T2B
A(1)	0.46	0.03	0.65	0.40
A(2)	0.53	0.03	0.74	0.45
A(3)	0.38	0.04	0.74	0.39
A(5)	0.06	-0.01	0.10	0.04
A(6)	0.36	0.10	0.38	0.30
A(7)	0.55	0.06	0.77	0.43
A(8)	0.40	0.13	0.42	0.20
A(9)	0.56	0.04	0.77	0.39
A(10)	0.55	0.03	0.74	0.39
A(11)	0.48	-0.01	0.71	0.42
A(12)	0.46	0.12	0.41	0.25
A(13)	0.46	0.12	0.52	0.23
A(14)	0.46	0.09	0.62	0.32
A(15)	0.33	0.10	0.39	0.23
A(16)	0.59	0.09	0.79	0.33
A(17)	0.48	0.36	0.24	0.18
A(18)	0.07	0.04	0.10	0.01
A(19)	0.59	0.07	0.74	0.33
A(20)	0.36	0.07	0.56	0.36
A(21)	0.48	0.09	0.65	0.33
A(22)	0.22	-0.04	0.20	0.17
A(23)	0.23	0.03	0.25	0.13
A(24)	0.26	0.00	0.25	0.13
A(25)	0.25	0.09	0.26	0.22
A(26)	0.56	0.03	0.79	0.36

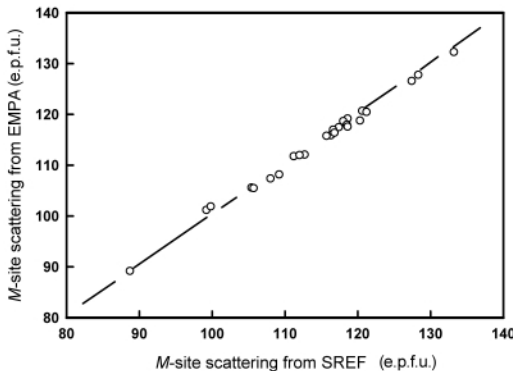


FIG. 5. Total M -site scattering from EMPA as a function of total M -site scattering from SREF (Structure REFinement); the line shows the 1:1 relation.

$$\text{Fig. 6: } \langle M^{1,2,3}-\text{O} \rangle = 1.4684 + 0.8553 \langle r^{M^{1,2,3}} \rangle.$$

This agreement indicates that the unit formulae are in good stereochemical accord with the refined crystal structures. Hence the M -site contents of Table 3 may be used in the assignment of the M -site populations (after normalization to complete occupancy of the M - (and T -) site contents). Inspection of the individual $\langle M-\text{O} \rangle$ distances (Table 5) shows that $\langle M2-\text{O} \rangle$ is generally much smaller than $\langle M1-\text{O} \rangle$ and $\langle M3-\text{O} \rangle$ in ${}^{[6]}\text{Al}$ -rich crystals, indicating that ${}^{[6]}\text{Al}$ tends to be ordered at the $M2$ site. Moreover, by analogy with non-dehydroxylated monoclinic amphiboles, we expect any Fe^{3+} present to occur at the $M2$ site. Thus we will start with examination of the $M2$ site.

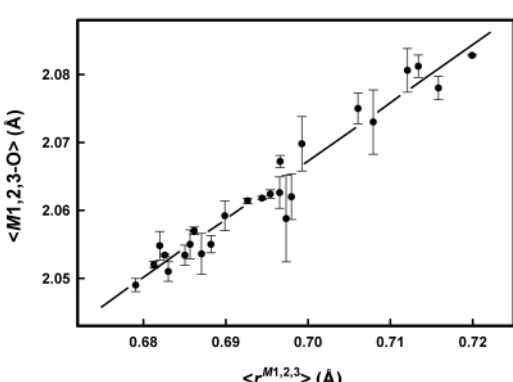


FIG. 6. Variation in $\langle M^{1,2,3}-\text{O} \rangle$ distance as a function of mean constituent-cation radius in orthorhombic amphiboles: the solid line is a least-squares fit to the data.

The $M2$ site

All octahedrally coordinated trivalent and tetravalent cations are assigned to $M2$, and we can calculate preliminary Mg and Fe^{2+} site-populations from the refined site-scattering value at the $M2$ site. Figure 7 shows the variation in $\langle M2-\text{O} \rangle$ as a function of aggregate radius of the constituent $M2$ cations. There is a well developed linear relation: $\langle M2-\text{O} \rangle = 1.447 + 0.899 \langle r^{M2} \rangle$, $R = 0.992$, $s_e = 0.004$; the slope of ~ 0.90 is to be compared with the slope of ~ 0.85 for the analogous relation in monoclinic amphiboles (Hawthorne and Oberti, 2007). The high correlation strongly supports the assigned site populations at the $M2$ site (Table 9), particularly the assigned Fe^{3+} contents.

The $M1$ and $M3$ sites

There is no evidence that either $M1$ or $M3$ is occupied by cations other than Mg and Fe^{2+} , or that O(3) has significant contents (of F, Cl or O) other than (OH). Hence we may calculate the Mg and Fe^{2+} contents of $M1$ and $M3$ directly from the site-scattering values of Table 6, as discussed above; resulting site-populations are given in Table 9.

The $M4$ site

In the amphiboles of the anthophyllite-gedrite series, the $M4$ site is occupied by Fe^{2+} and Mg, with minor Mn^{2+} , Ca and Na. Thus we assign

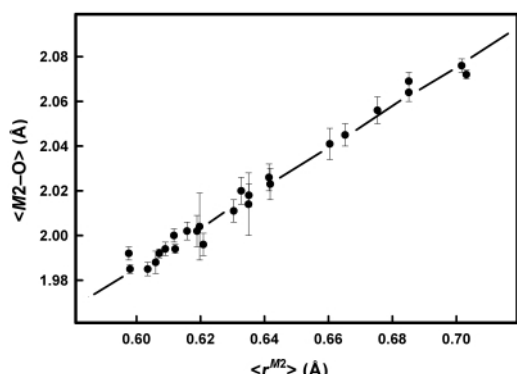


FIG. 7. Variation in $\langle M2-\text{O} \rangle$ distance as a function of mean constituent $M2$ -cation radius in orthorhombic amphiboles: the solid line is a least-squares fit to the data.

TABLE 9. Assigned site-populations in orthorhombic amphiboles.

	- M1 -		M2			- M3 -		M4			A			
	Mg	Fe ²⁺	Al	Ti	Mg	Fe ²⁺	Fe ³⁺	Mg	Fe ²⁺	Mn ²⁺	Ca	Fe ²⁺	Mg	Na
A(1)	1.59	0.41	1.15	0.01	0.76	0.00	0.08	0.77	0.23	0.00	0.02	1.23	0.75	0.44
A(2)	1.39	0.61	1.27	0.03	0.61	0.00	0.09	0.63	0.37	0.01	0.02	1.36	0.61	0.54
A(3)	1.20	0.80	1.04	0.02	0.81	0.04	0.09	0.54	0.46	0.03	0.01	1.67	0.29	0.38
A(5)	1.83	0.17	0.19	0.01	1.76	0.04	0.00	0.95	0.05	0.05	0.09	1.39	0.47	0.04
A(6)	1.62	0.38	0.85	0.04	0.98	0.00	0.13	0.76	0.24	0.01	0.05	1.45	0.49	0.27
A(7)	1.39	0.61	1.23	0.02	0.56	0.00	0.19	0.63	0.37	0.03	0.04	1.30	0.63	0.50
A(8)	1.40	0.60	0.85	0.03	0.92	0.09	0.11	0.74	0.26	0.01	0.05	1.16	0.78	0.27
A(9)	1.36	0.64	1.21	0.03	0.57	0.00	0.19	0.65	0.35	0.03	0.04	1.31	0.62	0.49
A(10)	1.39	0.61	1.14	0.02	0.64	0.00	0.20	0.64	0.36	0.06	0.04	1.35	0.55	0.52
A(11)	0.96	1.04	1.03	0.03	0.65	0.09	0.20	0.54	0.46	0.05	0.03	1.52	0.40	0.38
A(12)	1.39	0.61	0.87	0.04	0.90	0.08	0.11	0.73	0.27	0.01	0.05	1.15	0.79	0.27
A(13)	1.90	0.10	0.84	0.01	1.13	0.00	0.02	0.98	0.02	0.00	0.02	0.15	1.83	0.36
A(14)	1.44	0.56	1.13	0.01	0.74	0.06	0.06	0.76	0.24	0.00	0.02	1.03	0.95	0.47
A(15)	1.60	0.40	0.85	0.03	1.05	0.03	0.04	0.85	0.15	0.03	0.08	0.81	1.08	0.34
A(16)	1.23	0.77	1.21	0.02	0.58	0.04	0.15	0.65	0.35	0.06	0.04	1.16	0.74	0.56
A(17)	1.37	0.63	0.59	0.02	1.11	0.13	0.15	0.72	0.28	0.03	0.07	1.23	0.67	0.40
A(18)	1.68	0.32	0.20	0.01	1.62	0.17	0.00	0.86	0.14	0.05	0.10	1.02	0.83	0.05
A(19)	1.25	0.75	1.33	0.03	0.53	0.01	0.10	0.64	0.36	0.01	0.02	1.17	0.80	0.51
A(20)	1.74	0.26	0.97	0.03	0.94	0.06	0.00	0.88	0.12	0.02	0.08	1.00	0.90	0.36
A(21)	1.09	0.91	1.02	0.02	0.74	0.10	0.12	0.58	0.42	0.02	0.02	1.39	0.57	0.33
A(22)	1.68	0.32	0.49	0.01	1.40	0.01	0.09	0.84	0.16	0.00	0.04	1.64	0.32	0.22
A(23)	1.58	0.42	0.42	0.02	1.36	0.14	0.06	0.81	0.19	0.05	0.08	1.06	0.81	0.18
A(24)	1.44	0.56	0.45	0.03	1.24	0.21	0.07	0.75	0.25	0.09	0.09	1.22	0.60	0.23
A(25)	1.88	0.12	0.58	0.02	1.36	0.00	0.04	0.96	0.04	0.01	0.12	0.92	0.95	0.21
A(26)	1.79	0.21	1.18	0.05	0.77	0.00	0.00	0.88	0.12	0.02	0.04	0.83	1.11	0.50

Mn²⁺ and Ca from the unit formula, together with sufficient Na to fill the site, and then calculate the Fe²⁺ and Mg contents from the refined site-scattering values; values are given in Table 9.

The A site

The A site is occupied by Na that does not often exceed 0.50 a.p.f.u. The refined and EMPA contents of the A site, expressed in e.p.f.u., are compared in Fig. 8. Again, the agreement is quite close, and we assign the A-site populations as [⁴Na_{SREF} + Na_{EMPA}]/2. Site populations are given in Table 9. In some of the crystals, a small amount of positional disorder was present at the A site; weak subsidiary maxima were present. These maxima were included in the structure refinement in order to represent all of the scattering in the A cavity (hence the close agreement in Fig. 8); however, no pattern of disorder could be readily discerned. It seems likely that this disorder is associated with the partial unmixing of anthophyllite and gedrite components, and will be

affected both by the bulk composition of the crystal and by the degree and coarseness of the unmixing.

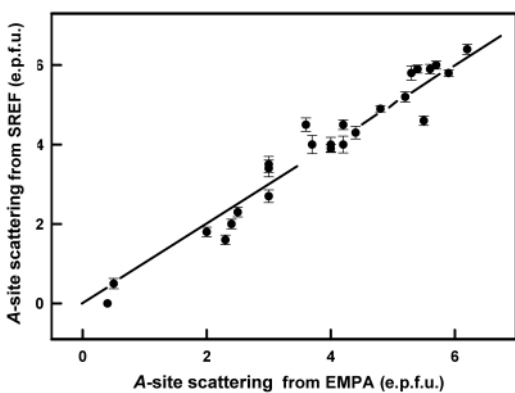


FIG. 8. Variation in A-site scattering from SREF (Structure REFinement) as a function of A-site scattering from EMPA; the line shows the 1:1 relation.

Summary

(1) Despite the problems in unmixing due to the low-temperature solvus present in the anthophyllite–gedrite series (Spear, 1980), we have obtained reasonably good refinement results on amphiboles along this series.

(2) The grand $\langle T-O \rangle$ distance is related to the T_{Al} content (in a.p.f.u.) by the relation

$$\langle\langle T-O \rangle\rangle = 1.6215(9) + 0.0173(6) [{}^4\text{Al}]$$

(3) Tetrahedrally coordinated Al shows the following pattern of order: $T1\text{B} > T2\text{B} > T1\text{A} > T2\text{A}$.

(4) The grand $\langle M^{1,2,3}-O \rangle$ distance is related to the mean radius of the constituent cations, $\langle r^{M1,2,3} \rangle$, by the relation

$$\langle\langle M^{1,2,3}-O \rangle\rangle = 1.4684 + 0.8553 \langle r^{M1,2,3} \rangle.$$

(5) Octahedrally coordinated Al is ordered at the $M2$ site.

(6) Mössbauer spectroscopy indicates small (0.00–0.20 a.p.f.u.) amounts of Fe^{3+} present, and these were assigned to the $M2$ site; the resultant $M2$ site populations give a well developed linear relation ($\langle M2-O \rangle = 1.447 + 0.899 \langle r^{M2} \rangle$, $R = 0.992$, see 0.004 Å) between mean bond length and constituent-cation radius at the $M2$ site.

(7) Mg and Fe^{2+} are fairly evenly distributed between the $M1$ and $M3$ sites.

Acknowledgements

FCH was supported by a Canada Research Chair in Crystallography and Mineralogy and Research Tools and Equipment, Discovery and Major Facilities Access grants from the Natural Sciences and Engineering Research Council of Canada. BWE was supported by U.S. National Science Foundation grant EAR 97-06326.

References

- Bancroft, G.M. and Burns, R.G. (1968) Applications of the Mössbauer effect to mineralogy. Pp. 36–42 in: *Papers and Proceedings of the Fifth General Meeting of the International Mineralogical Association (Cambridge, 1966)*. Mineralogical Society, London.
- Bancroft, G.M., Maddock, A.G., Burns, R.G. and Strens, R.G.J. (1966) Cation distribution in anthophyllite from Mössbauer and infrared spectroscopy. *Nature*, **212**, 913–915.
- Bancroft, G.M., Maddock, A.G. and Burns, R.G. (1967) Applications of the Mössbauer effect to silicate mineralogy. I. Iron silicates of known crystal structure. *Geochimica et Cosmochimica Acta*, **31**, 2219–2246.
- Barabanov, A.V. and Tomilov, S.B. (1973) Mössbauer study of the isomorphous series anthophyllite–gedrite and cummingtonite–grunerite. *Geochemistry International USSR*, 1240–1247.
- Berg, J.H. (1985) Chemical variations in sodium gedrite from Labrador. *American Mineralogist*, **70**, 1205–1210.
- Burns, R.G. and Law, A.D. (1970) Hydroxyl stretching frequencies in the infrared spectra of anthophyllites and gedrites. *Nature*, **226**, 73–75.
- Champness, P.E. and Rodgers, K.A. (2000) The origin of iridescence in anthophyllite–gedrite from Simiutat, Nuuk district, southern West Greenland. *Mineralogical Magazine*, **64**, 885–889.
- Claeson, D.T. and Meurer, W.P. (2002) An occurrence of igneous orthorhombic amphibole, Eriksberg gabbro, southern Sweden. *American Mineralogist*, **87**, 699–708.
- Evans, B.W., Ghiorso, M.S., Yang, H. and Medenbach, O. (2001) Thermodynamics of the amphiboles: Anthophyllite–ferroanthophyllite and the ortho-clino phase loop. *American Mineralogist*, **86**, 640–651.
- Fabriès, J. and Perseil, E.A. (1971) Nouvelles observations sur les amphiboles orthorhombiques. *Bulletin de la Société française Minéralogie et de Cristallographie*, **94**, 385–395.
- Finger, I.W. (1970) Refinement of the crystal structure of an anthophyllite. *Carnegie Institute of Washington Year Book*, **68**, 283–288.
- Gittos, M.F., Lorimer, G.W. and Champness, P.E. (1976) The phase distribution of exsolved amphiboles. Pp. 238–247 in: *Electron Microscopy in Mineralogy* (H.R. Wenk, editor). Springer, New York.
- Hawthorne, F.C. (1983) The crystal chemistry of the amphiboles. *The Canadian Mineralogist*, **21**, 173–480.
- Hawthorne, F.C. and Oberti, R. (2007) Amphiboles: Crystal chemistry. Pp. 1–54 in: *Amphiboles: Crystal Chemistry, Occurrence and Health Issues* (F.C. Hawthorne, R. Oberti, G. Della Ventura and A. Mottana, editors). Reviews in Mineralogy and Geochemistry **67**, Mineralogical Society of America, Chantilly, VA, and the Geochemical Society, Washington, D.C.
- Hirschmann, M., Evans, B.W. and Yang, H. (1994) Composition and temperature dependence of Fe–Mg ordering in cummingtonite–grunerite as determined by X-ray diffraction. *American Mineralogist*, **79**, 862–877.
- Ibers, J.A. and Hamilton, W.C. (eds.) (1992) *International Tables for X-ray Crystallography IV*. Kynoch Press, Birmingham, U.K.
- Ishida, K. (1998) Cation disordering in heat-treated

- anthophyllites through oxidation and dehydrogenation. *Physics and Chemistry of Minerals*, **25**, 160–167.
- Ishida, K. and Hawthorne, F.C. (2003) Fine structure in the infrared OH-stretching bands of holmquistite and anthophyllite. *Physics and Chemistry of Minerals*, **30**, 330–336.
- Ito, T. and Morimoto, N. (1950) Anthophyllite. Pp. 42–49 in: *X-ray studies on Polymorphism* (T. Ito, R. Sadanaga and Y. Takéuchi, editors). Maruzen Co. Ltd., Tokyo.
- Law, A.D. (1976) A model for the investigation of hydroxyl spectra of amphiboles. Pp. 677–686 in: *The Physics and Chemistry of Minerals and Rocks* (R.G.J. Strens, editor). John Wiley and Sons, London.
- Law, A.D. (1981) Studies of the orthoamphiboles. II. Hydroxyl spectra of anthophyllites. *Bulletin de la Société française Minéralogie et de Cristallographie*, **104**, 423–430.
- Law, A.D. (1982) Studies of the orthoamphiboles. III. Hydroxyl spectra of gedrites. *Mineralogical Magazine*, **45**, 63–71.
- Law, A.D. (1989) Studies of the orthoamphiboles. IV. Mössbauer spectra of anthophyllites and gedrites. *Mineralogical Magazine*, **53**, 181–191.
- Leake, B.E., Woolley, A.R., Arps, C.E.S., Birch, W.D., Gilbert, M.C., Grice, J.D., Hawthorne, F.C., Kato, A., Kisch, H.J., Krivovichev, V.G., Linthout, K., Laird, J., Mandarino, J.A., Maresch, W.V., Nickel, E.H., Rock, N.M.S., Schumacher, J.C., Smith, D.C., Stephenson, N.C.N., Ungaretti, L., Whittaker, E.J.W. and Youshi, G. (1997) Nomenclature of Amphiboles: Report of the Subcommittee on Amphiboles of the International Mineralogical Association, Commission on New Minerals and Mineral Names. *Mineralogical Magazine*, **61**, 295–321.
- Lindemann, W. (1964) Beitrag zur Struktur des Anthophyllits. *Fortschritte der Mineralogie*, **42**, 205 (abstract).
- Mao, H.K. and Seifert, F. (1974) A study of the crystal-field effects of iron in the amphiboles anthophyllite and gedrite. *Carnegie Institute of Washington Year Book*, **73**, 500–502.
- Müller, W.F., Schmädicke, E., Okrusch, M. and Schüssler, U. (2003) Intergrowths between anthophyllite, gedrite, calcic amphibole, cummingtonite, talc and chlorite in a metamorphosed ultramafic rock of the KTB pilot hole, Bavaria. *European Journal of Mineralogy*, **15**, 295–307.
- Oberti, R., Ungaretti, L., Cannillo, E., Hawthorne, F.C. and Memmi, I. (1995) Temperature-dependent Al order-disorder in the tetrahedral double-chain of *C2/m* amphiboles. *European Journal of Mineralogy*, **7**, 1049–1063.
- Papike, J.J. and Ross, M. (1970) Gedrites: crystal structures and intracrystalline cation distributions. *American Mineralogist*, **55**, 1945–1972.
- Rabbit, J.C. (1948) A new study of the anthophyllite series. *American Mineralogist*, **33**, 263–323.
- Rancourt, D.G. and Ping, J.Y. (1991) Voigt-based methods for arbitrary-shape static hyperfine parameter distributions in Mössbauer spectroscopy. *Nuclear Instruments and Methods in Physics Research*, **B58**, 85–97.
- Robinson, P. and Jaffe, H.W. (1969) Chemographic exploration of amphibole assemblages from central Massachusetts and southwestern New Hampshire. *Mineralogical Society of America Special Paper*, **2**, 251–274.
- Robinson, P., Ross, M. and Jaffe, H.W. (1971) Composition of the anthophyllite-gedrite series, comparisons of gedrite-hornblende, and the anthophyllite-gedrite solvsus. *American Mineralogist*, **56**, 1004–1041.
- Robinson, P., Spear, F.S., Schumacher, J.C., Laird, J., Klein, C., Evans, B.W. and Doolan, B.L. (1981) Phase relations of metamorphic amphiboles: natural occurrence and theory. Pp. 1–227 in: *Amphiboles. Petrology and Experimental Phase Relations* (D.R. Veblen and P.H. Ribbe, editors). Reviews in Mineralogy **9B**, Mineralogical Society of America, Washington, D.C.
- Schneidermann, J.S. and Tracy, R.J. (1991) Petrology of orthoamphibole-cordierite gneisses from the Orijärvi area, southwest Finland. *American Mineralogist*, **76**, 942–955.
- Schumacher, J. and Robinson, P. (1987) Mineral chemistry and metasomatic growth of aluminous enclaves in gedrite-cordierite-gneiss from southwestern New Hampshire, U.S.A. *Journal of Petrology*, **28**, 1033–1073.
- Seifert, F. (1977) Compositional dependence of the hyperfine interaction of 5Fe in anthophyllite. *Physics and Chemistry of Minerals*, **1**, 43–52.
- Seifert, F. (1978) Equilibrium Mg-Fe²⁺ cation distribution in anthophyllite. *American Journal of Science*, **278**, 1323–1333.
- Seifert, F. and Virgo, D. (1974) Temperature dependence of intracrystalline Fe²⁺-Mg distribution in a natural anthophyllite. *Carnegie Institute of Washington Year Book*, **73**, 405–411.
- Shannon, R.D. (1976) Revised effective ionic radii and systematic studies of interatomic distances in halides and chalcogenides. *Acta Crystallographica*, **A32**, 751–767.
- Sheldrick, G.M. (1997) *SHELX-97: Program for the solution and refinement of crystal structures*. Siemens Energy and Automation, Madison, WI.
- Sheldrick, G.M. (1998) *SADABS User Guide*, University of Göttingen, Germany.

- Smelik, E.A. and Veblen, D.R. (1993) A transmission and analytical electron microscope study of exsolution microstructures in the orthoamphiboles anthophyllite and gedrite. *American Mineralogist*, **78**, 511–532.
- Spear, F.S. (1980) The gedrite-anthophyllite solvus and the composition limits of orthoamphibole from the Post Pond Volcanics, Vermont. *American Mineralogist*, **65**, 1103–1118.
- Stout, J.H. (1971) Four coexisting amphiboles from Telemark, Norway. *American Mineralogist*, **56**, 212–224.
- Strens, R.G.J. (1966) Infrared study of cation ordering and clustering in some (Fe,Mg) amphibole solid solutions. *Chemical Communications*, **15**, 519–520.
- Strens, R.G.J. (1974) The common chain, ribbon and ring silicates. Pp. 305–344 in: *The Infrared Spectra of Minerals* (V.D. Farmer, editor). Mineralogical Society, London.
- Stroink, G., Blaauw, C., White, C.G. and Leiper, W. (1980) Mössbauer characteristics of UICC standard reference asbestos samples. *The Canadian Mineralogist*, **18**, 285–290.
- Treloar, P.J. and Putnis, A. (1982) Chemistry and microstructure of orthoamphiboles from cordierite-amphibole rocks at Outokumpu, North Karelia, Finland. *Mineralogical Magazine*, **45**, 55–62.
- Walitz, E.M., Walter, F. and Ettinger, K. (1989) Verfeinerung der Kristallstruktur von Anthophyllit vom Ochsenkogel/Gleinalpe, Österreich. *Zeitschrift für Kristallographie*, **188**, 237–244.
- Warren, B.E. and Modell, D.I. (1930) The structure of anthophyllite $H_2Mg_7(SiO_3)_8$. *Zeitschrift für Kristallographie*, **75**, 161–178.